Ring-Based Syncr. Light Sources: A Deterministic Approach

Johan Bengtsson

June 23, 2015

Outline: “Engineering-Science”

Predictable Results:

- **First Principles: Global Optimization.**
- **Systematic Approaches.**
- **Robust Design and Control.**

Application to: Chasman-Green Lattices and Damping Wigglers.

Conclusions.

First Principles: Global Optimization (PAC 2007)

1. Horizontal emittance (natural): damping $\leftrightarrow$ diffusion (fundamental limit is IBS).

2. Optimize (for Insertion Devices, (EPAC 2008):

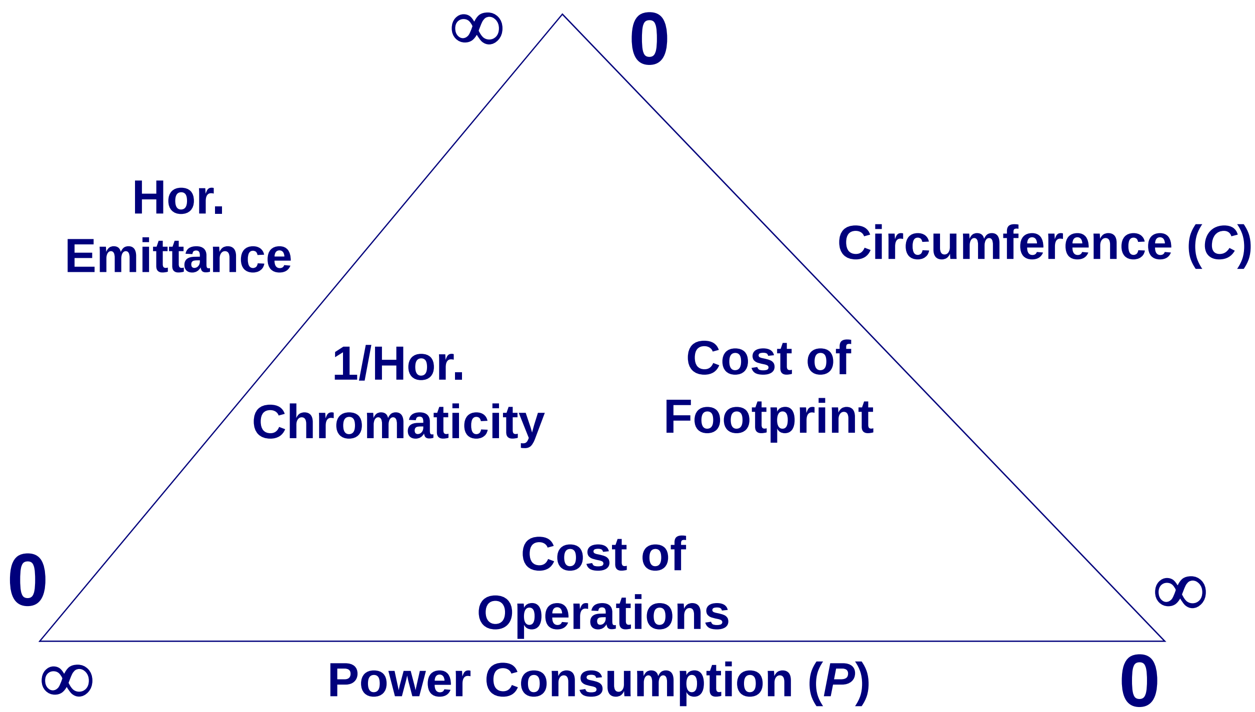

$$\varepsilon_x \sim \frac{1}{R^2 \cdot P},$$

R bend radius

Optics guidelines:

- max chromaticity per cell,
- min peak dispersion,
- max values for the beta functions.

Systematic Approaches

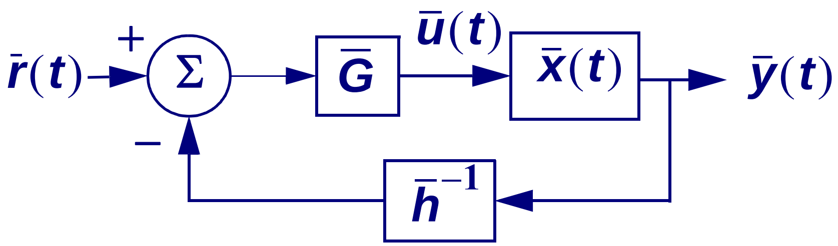

"Closed-Loop" Control:

- lattice design,
- control of DA,
- guidelines for engineering tolerances, ring magnets, and insertion devices,
- correction algorithms,
- aka TQM in industry.

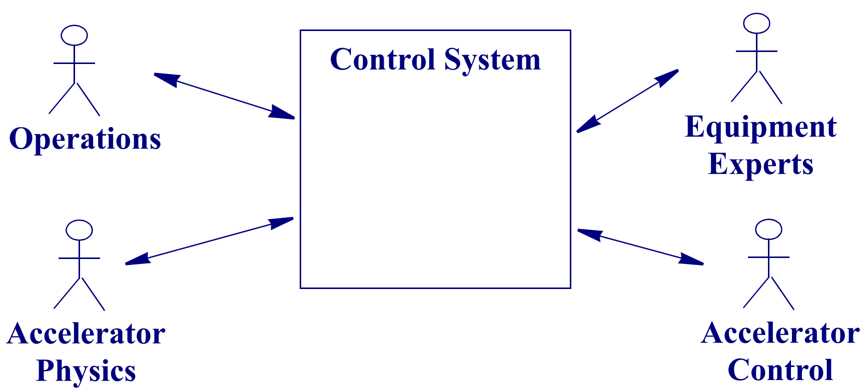

"<u>Use Case</u>" approach:

- model based control.

Robust Design and Control: Model Based (ICAP 2009)

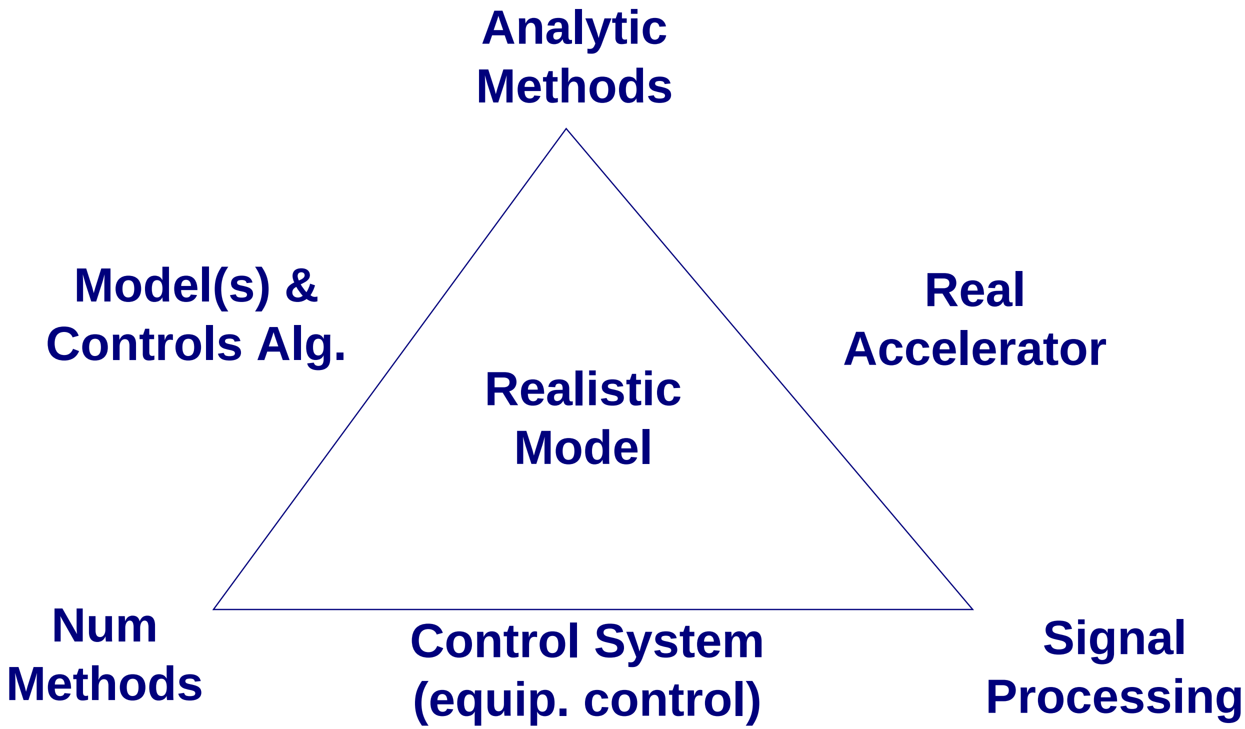

Challenge: re-use the design model for model based (on-line) control.

Chasman-Green Lattices and Damping Wigglers

[1] R. Chasman, G. Green, E. Rowe "Preliminary Design of a Dedicated Synchrotron Radiation Facility" PAC 1975.

[2] M. Sommer "Optimization of the Emittance of Electrons (Positrons) Storage Rings" LAL/RT/83-15 (1983).

[3] L. Teng "Minimum Emittance Lattice for Synchrotron Radiation Storage Rings" ANL LS-17 (1985).

[4] G. Vignola "The Use of Gradient Magnets in Low Emittance Electron Storage Rings" NIM 246A, 12-14 (1986) (-> ALS).

[5] H. Wiedemann "An Ultra-Low Emittance Mode for PEP Using Damping Wigglers" NIM 266A, 24-31 (1988).

[6] K. Balewski et al "PETRA III: A New High Brilliance Synchrotron Radiation Source at DESY" EPAC 2004.

[7] S. Ozaki et al "Philosophy for NSLS-II Design with Sub-Nanometer Horizontal Emittance" PAC 2007.

[8] G. Wang et al "Results of the NSLS-II Commissioning" APS, 2015.

Already 1985 Teng noted that (p. 18):

"This theoretical minimum should be at least a factor 2 smaller than the desired emittance because when one gets to the later steps, it is unlikely that one can attain and then maintain optimum values for all the parameters."

i.e., a system approach.

Ring-Based Syncr. Light Sources: Basics

The dynamic equilibrium for the horizontal emittance and momentum spread are

$$\varepsilon_x = \tau_x \langle \mathcal{H}_x \cdot D_\delta \rangle, \qquad \sigma_\delta^2 = \tau_E \langle D_\delta \rangle, \qquad \tau_E = \frac{2T_0}{J_\mathrm{E}} \frac{E_0}{U_\mathrm{tot}}, \qquad \tau_x = \frac{2}{J_x} \tau_E .$$

where (linear dispersion action)

$$\mathcal{H}_x \equiv \tilde{\eta}^\mathrm{T} \tilde{\eta}, \qquad \bar{\eta} \equiv \begin{bmatrix} \eta_x \\ \eta'_x \end{bmatrix}, \qquad \tilde{\eta} \equiv A^{-1} \bar{\eta}, \qquad A^{-1} = \begin{bmatrix} 1/\sqrt{\beta_x} & 0 \\ \alpha_x/\sqrt{\beta_x} & \sqrt{\beta_x} \end{bmatrix}$$

The partition numbers are governed by ("sum rule", Robinson, 1958)

$$J_x + J_y + J_\mathrm{E} = 4$$

No dipole gradients => $J_x \approx 1, J_E \approx 2$.

Ring-Based Syncr. Light Source: Basics (cont.)

The dynamic quantities can be expressed in terms of the global linear optics properties for the lattice (Sands, 1970)

$$\varepsilon_x = \tau_x \langle \mathcal{H}_x \cdot D_\delta \rangle = \frac{C_q \gamma^2}{J_x} \frac{\langle \mathcal{H}_x / |\rho|^3 \rangle_0}{\langle 1/\rho^2 \rangle_0}, \qquad \sigma_\delta^2 = \frac{C_q \gamma^2}{J_E} \frac{\langle 1/|\rho|^3 \rangle_0}{\langle 1/\rho^2 \rangle_0}, \qquad C_q = \frac{55}{32\sqrt{3}} \frac{\hbar}{m_e c_0}$$

i.e., convenient for linear optics design.

For an isomagnetic lattice

$$\varepsilon_x\ [\mathrm{nm \cdot rad}] = 7.84 \times 10^3 \cdot \frac{(E\ [\mathrm{GeV}])^2 F}{J_x N_d^3}$$

where N_d is the number of dipoles and $F \geq 1$.

The equilibrium can be shifted by introducing Damping Wigglers (DWs)

$$\frac{\varepsilon_{xw}}{\varepsilon_{x0}} = \frac{1 + \langle \mathcal{H}_x / |\rho|^3 \rangle_w / \langle \mathcal{H}_x / |\rho|^3 \rangle_0}{1 + \langle 1/\rho^2 \rangle_w / \langle 1/\rho^2 \rangle_0} \approx \frac{U_0}{U_0 + U_w}, \qquad \frac{\sigma_{\delta_w}}{\sigma_{\delta_0}} = \sqrt{\frac{1 + \frac{8}{3\pi} \frac{B_w}{B_0} \frac{U_w}{U_0}}{1 + \frac{U_w}{U_0}}}.$$

Ring-Based Syncr. Light Source: Basics (cont.)

For a fixed number of dipoles, it follows that

$$\varepsilon_x \sim \frac{\langle \mathcal{H}_x / |\rho|^3 \rangle_0}{\langle 1/\rho^2 \rangle_0} \frac{U_0}{U_0 + U_w} \sim \frac{1}{\rho_0^2 U_{tot}}$$

where P is the total radiated power.

Hence, apart from IBS (Intra Beam Scattering), there is no “sho w stopper” for a diffraction limited ring-based synchrotron light source.

Clearly, PETRA III, NSLS-II, and MAX-IV (R&D by MAX-III) have “paved the way”; i.e., how to avoid the “chromaticity wall”. An artifact originating from the TME (“Theoretical” Minimum Emittance) cell; reductionism vs. “engineering-science”.

The circumference for a few existing facilities are:

Facility	Circ. [km]	E [GeV]
ESRF	0.84	6
APS	1.1	7
SPRING-8	1.4	8
PEP X	2.2	4.5
PETRA III	2.3	6

vs. "A Common Mistake" (M. Borland, FLS 2010)

Emittance of Electron Storage Rings[1]

- Quantum excitation causes emittance growth in any bending system

$$\left(\frac{d}{dt}\langle\epsilon\rangle\right)_q \approx \frac{\langle \dot{N}_{ph}\langle u_\gamma^2\rangle \mathcal{H}(s)\rangle_s}{2E_0^2} \propto E_0^5$$

$$\mathcal{H} = \beta_x \eta_x'^2 + 2\alpha_x \eta_x \eta_x' + \frac{1+\alpha_x^2}{\beta_x}\eta_x^2$$

- Fortunately, in electron rings there is also damping

$$\left(\frac{d}{dt}\langle\epsilon\rangle\right)_d \approx -\frac{\langle P_\gamma\rangle}{E_0}\epsilon \propto E_0^3$$

- Giving the equilibrium emittance

$$\epsilon \propto E_0^2 \frac{\langle \mathcal{H}/\rho^3\rangle}{\langle 1/\rho^2\rangle}$$

- A common mistake

$$\epsilon \propto \frac{E_0^2}{R}$$

Wrong!

[1] H. Wiedemann, Particle Accelerator Physics.

A Perspective (ESRF, LEL 2015)

LOW EMITTANCE RINGS TREND

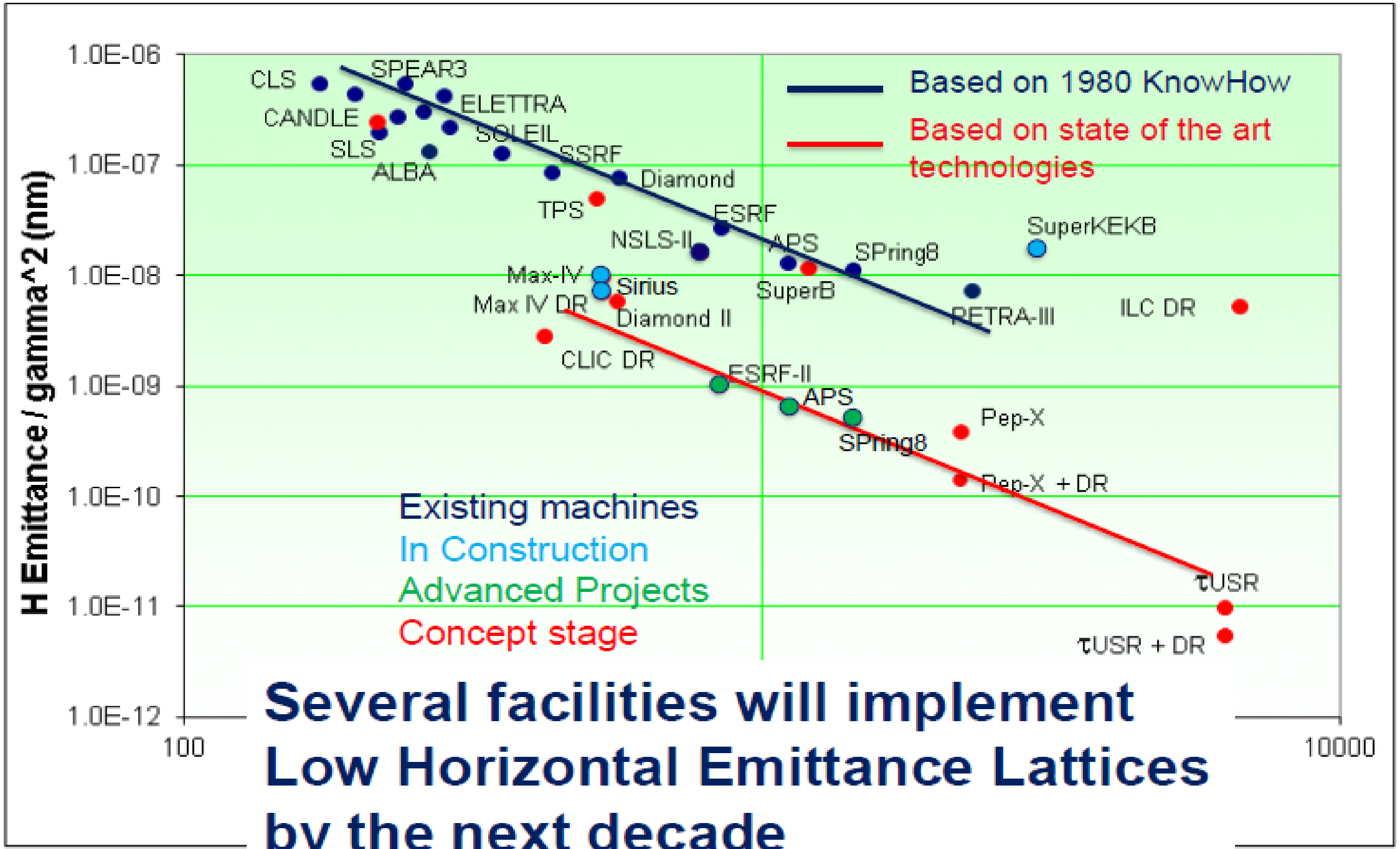

Several facilities will implement Low Horizontal Emittance Lattices by the next decade

The European Synchrotron | ESRF

A Measure for Stiffness of Chrom. Ctrl (ICFA 57, 2012)

3.6.5 The Chromatic Control Problem: A Measure for Stiffness

It is known that (fixed ρ_b) [36]

$$\varepsilon_x[\text{nm}\cdot\text{rad}] = 1470 \cdot \frac{(E\,[\text{GeV}])^2 \langle \mathcal{H}_x \rangle^{\min}}{\rho_b J_x} = 1470 \cdot \frac{(E\,[\text{GeV}])^2 (2\pi)^3 F}{12\sqrt{15} J_x N_b^3} \qquad (2)$$

where N_b is the total number of dipoles and [37]

$$F_{\text{CB}} = 1, \quad F_{\text{EB}} = 3, \quad F_{N\text{-BA}} = \left(\frac{N}{2 + (N-2) \cdot 3^{1/3}} \right)^3 F_{\text{EB}} \qquad (3)$$

for a "center bend", "end bend", and N-BA, respectively.

As a measure for the *stiffness* of the chromatic control problem, we introduce

$$S \equiv \frac{|\xi_x|}{\nu_x \sqrt{\langle \mathcal{H}_x \rangle}} \sim \frac{1}{\text{DA}}. \qquad (4)$$

Note that the DA has a minimum for the $\langle \mathcal{H}_x \rangle^{\min}$-cell. A survey of F_{rel} (= 1 for $\langle \mathcal{H}_x \rangle^{\min}$) vs. S is summarized in Tab. 1. For the operating facilities we find: $S = 49 \pm 23$.

A Measure for Stiffness of Chrom. Ctrl (cont.)

Table 1: Survey of F_{rel} vs. Stiffness S for some Storage-Ring Light Sources.

Lattice	Type	E [GeV]	ε_x [nm·rad]	ε^*_x [nm·rad]	J_x	$<\mathcal{H}_x>$ [$\times 10^{-3}$]	F_{rel}	ξ_x/ν_x	S
SPring-8	11×DB-4	8	3.4	3.7	1.0	1.42	4.6	2.2	58
ESRF	DB-32	6	3.8		1.0	1.68	3.5	3.6	89
APS	DB-40	7	2.5	3.1	1.0	1.35	3.3	2.5	69
PETRA III	Mod. FODO	6	1		1.0	3.62	39.8	1.2	20
SPEAR3	DB-18	3	11.2		1.0	5.73	7.4	5.5	73
ALS	TB-12	1.9	6.3	6.4	1.0	4.99	10.4	1.7	24
BESSY II	TBA-10	1.9	6.1		1.0	4.83	2.9	2.8	40
SLS	TBA-12	2.4	5		1.0	3.38	2.6	3.2	56
DIAMOND	DB-24	3	2.7		1.0	1.46	4.2	2.9	76
ASP	DB-14	3	7		1.4	5.60	3.0	2.1	28
ALBA	DB-16	3	4.3		1.3	2.96	2.6	2.1	39
SOLEIL	DB-16	2.75	3.7	5.5	1.0	1.79	2.0	2.8	67
CLS	DBA-12	2.9	18.3		1.6	16.79	2.0	1.3	10
ELETTRA	DBA-12	2	7.4		1.3	9.12	1.4	3.0	31
TPS	DB-24	3	1.7		1.0	1.08	2.7	2.9	87
NSLS-II	DBA-30	3	2		1.0	3.78	2.0	3.1	50
MAX-IV	7BA-20	3	0.33		1.9	0.40	18.1	1.2	59
PEP-X (TME)	4×8TME-6	4.5	0.095		1.0	0.34	3.3	1.7	90
PEP-X (USR)	8×7BA-6	4.5	0.029		1.0	0.10	5.3	1.4	145
TeVUSR	30×7BA-6	11	0.031		2.4	0.02	12.0	1.4	360
TeVUSR	30×7BA-6	9	0.029		2.7	0.02	18.4	1.4	281

The NSLS-II “Wind Tunnel” (BNL, 2006)

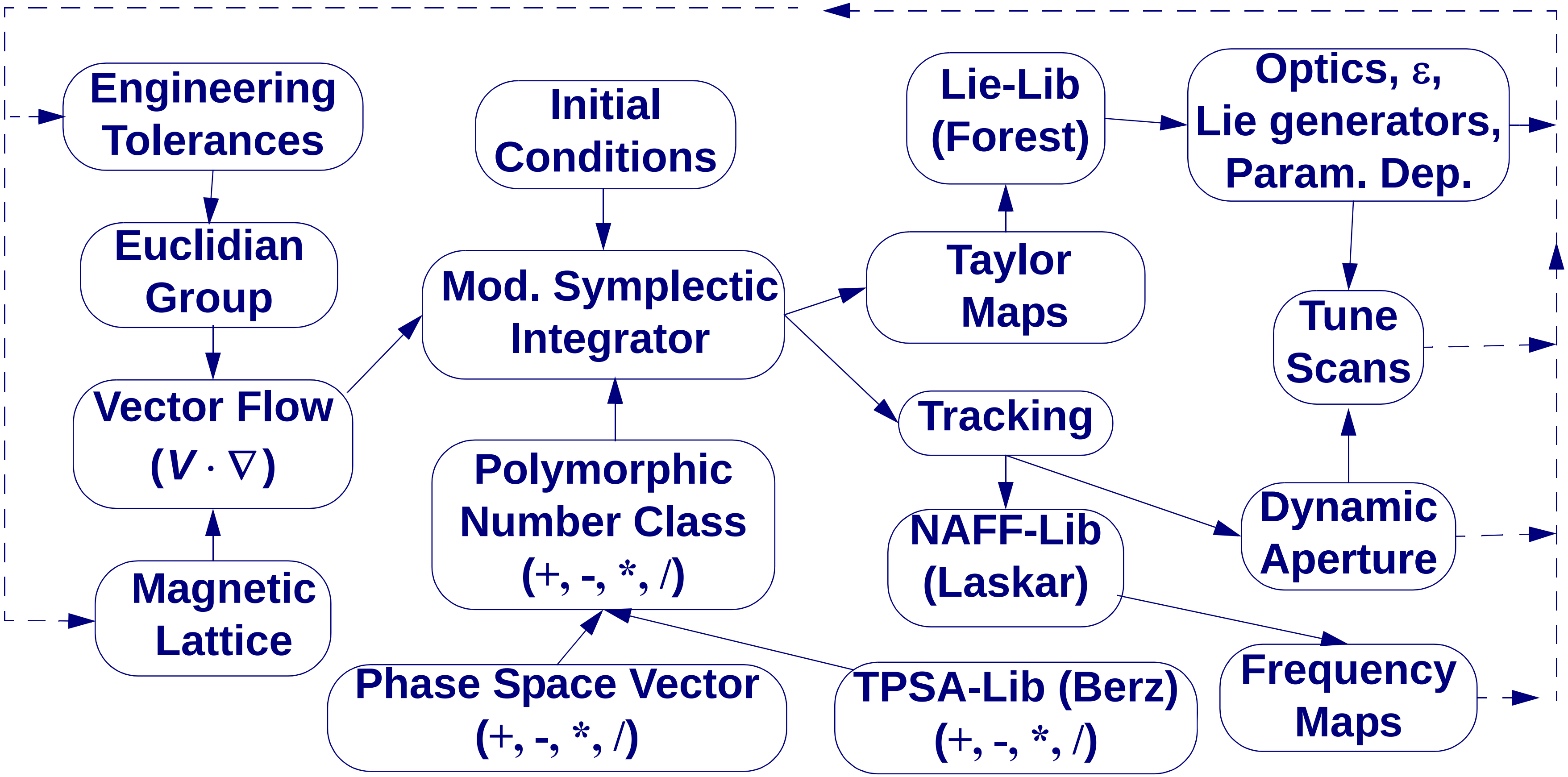

=> self-consistent: numerical simulations/analysis and analytic techniques applied to the same (realistic) model.

The NSLS-II "Wind Tunnel" (cont.)

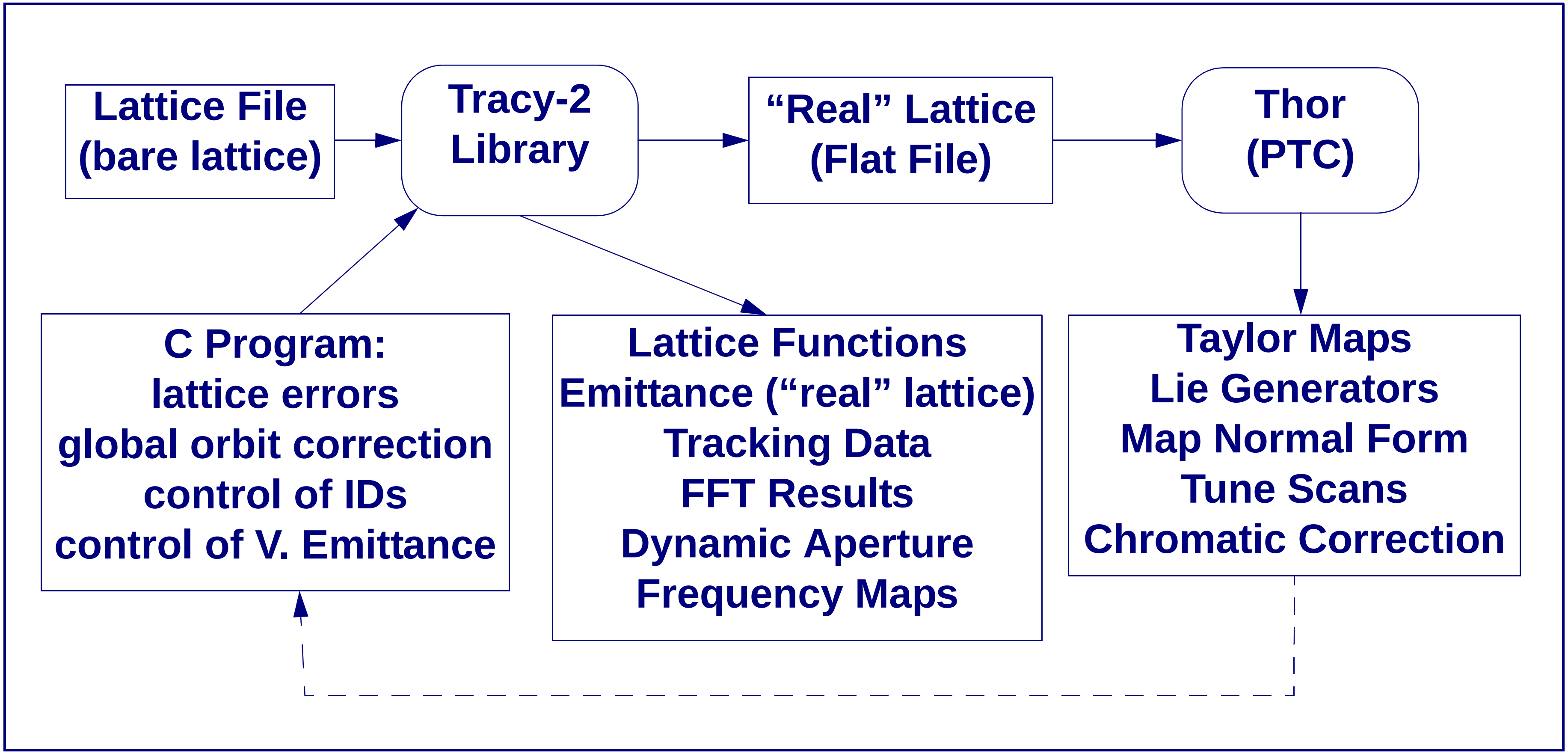

Implementation (~50,000 lines of C++, C, and FORTRAN code; two different codes, Tracy-2 in C and Thor in C++, at the time).

Lessons Learnt, ALS: Control of Orbit

EPAC 1988

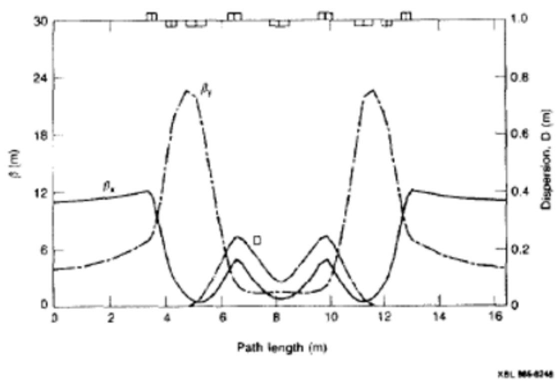

Fig. 3. Lattice functions through one unit cell of the TBA structure.

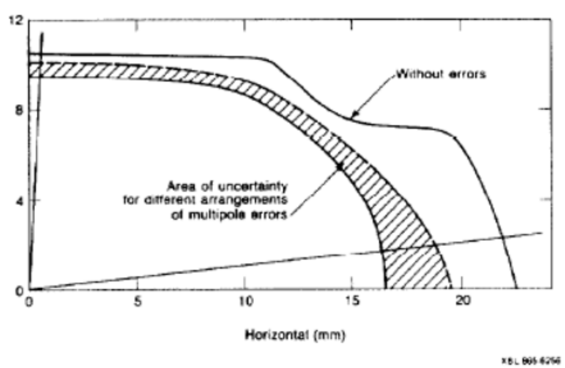

Fig. 5. Dynamic aperture in the presence of multipole errors.

For the linear optics see Vignola NIM 246A 1986.

D. Robin et al (EPAC 1996)

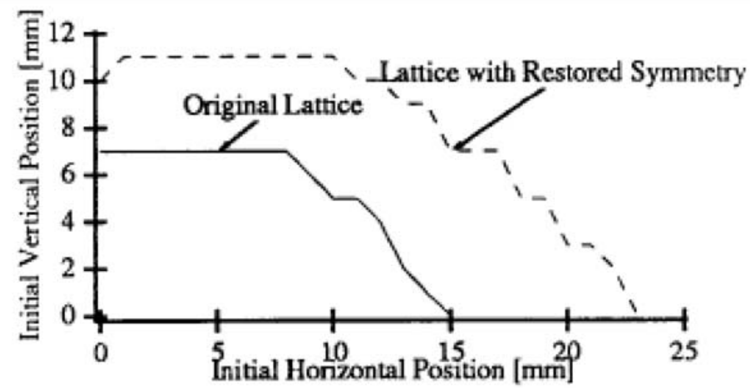

Figure 6: Comparison of dynamic aperture for the original and restored symmetry lattices.

- **Only 2 sextupole families.**
- **Orbit control not robust; not "tied down" in the sextupoles (BPM placement based on linear optics).**
- **For the "48-Knob Scheme" see AIP Conf. Proc. 255 (1991).**
- **For validation of the nonlinear model (Tracy-2), see J. Bengtsson et al (PAC 1994).**

Closing-the-Loop (EPAC 1994)

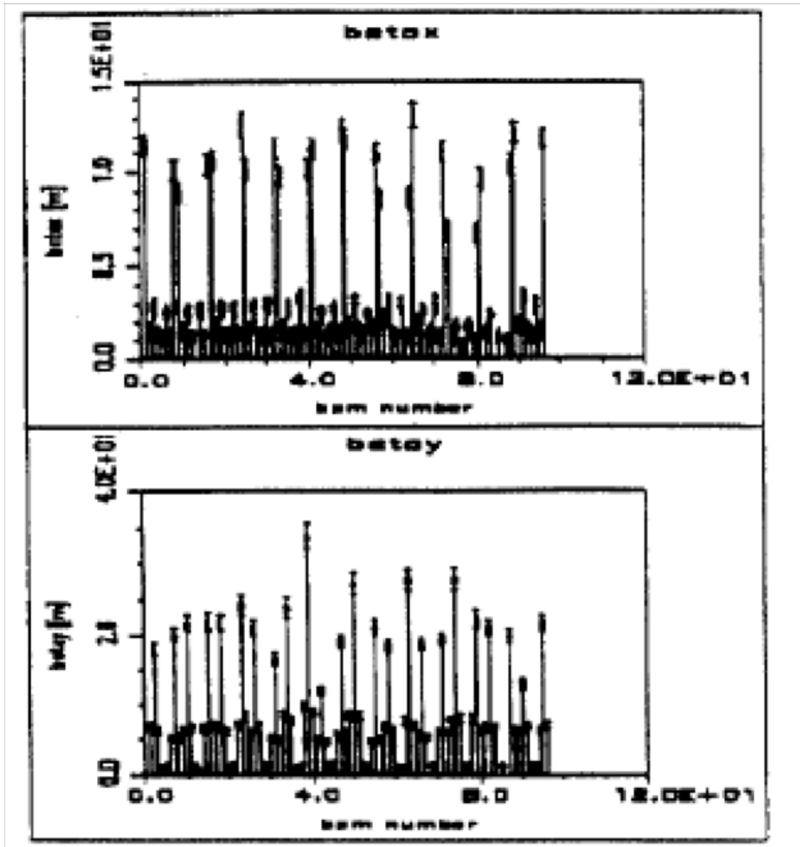

Fig.2 Estimated Beta Functions

component (no sextupole)	order	x	y
Tracy-2	1	-24.89	-26.84
	2	33.97	66.68
improved Tracy $(1/(1+\delta))$	1	-24.89	-27.88
	2	33.97	70.64
Krakpot prot	1	-24.59	-27.68
	2	32.66	74.18
Krakpot (prot, n.l. drift, quad.fringe)	1	-24.78	-27.66
	2	34.91	75.67

component (with sextupoles)	order	x	y
no higher order multipoles	1	1.00	-0.78
	2	-43.65	-67.86
all syst.higher order multipoles	1	1.00	-0.78
	2	-40.41	-57.28
only syst. octupole in Bend.	1	1.00	-0.78
	2	-45.03	-57.10

Lessons Learnt, SLS: Seven-BA-6

EPAC 1994

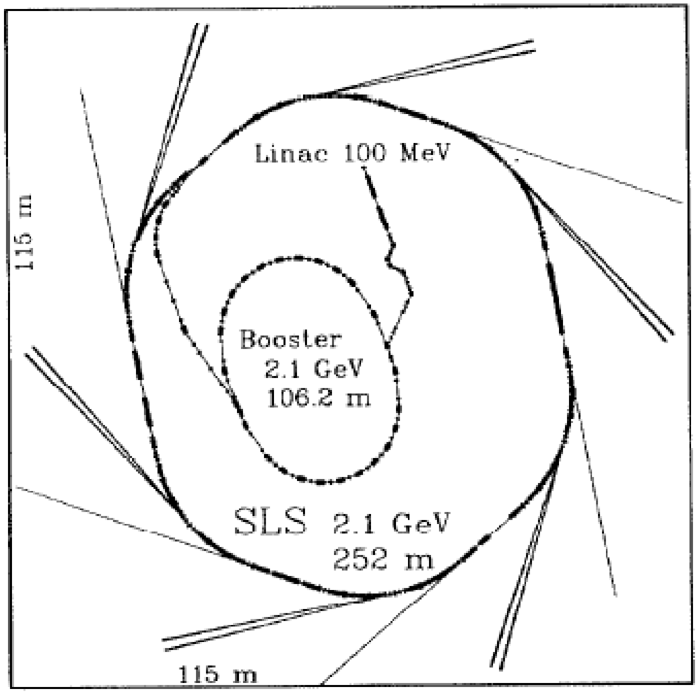

Figure 2: Layout of the SLS facility with linac, booster and storage ring. Shown are the photon beamlines from insertion devices and the twin beamlines from the six superconducting bending magnets.

EPAC 1996

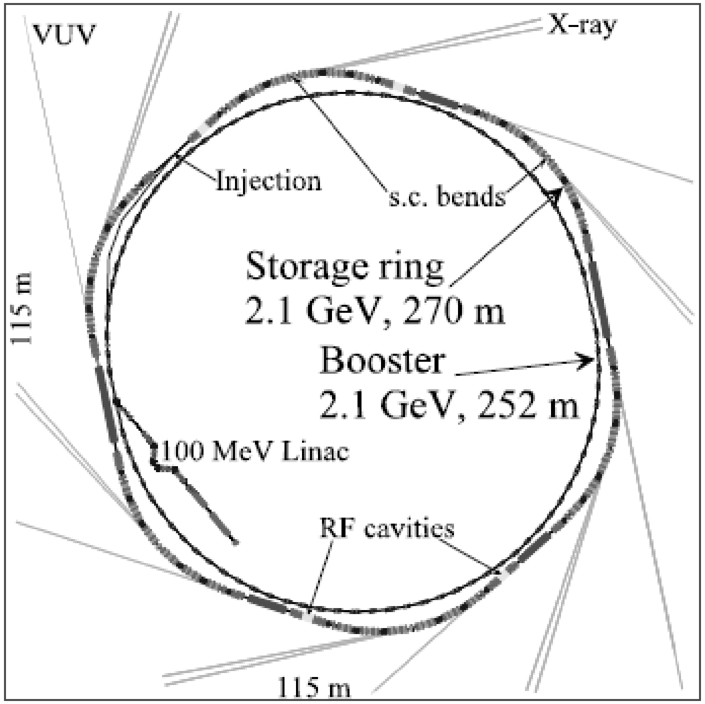

Figure 1: Layout of the SLS facility with linac, booster and storage ring. Shown are the possible photon beamlines from insertion devices and the possible twin beamlines from the six superconducting bending magnets.

For a perspective see:

1. **A. Streun "Nonlinear Dynamics at the SLS Storage Ring" LER 2010 (4 phase tromb. and 33 sext. fam.).**
2. **P. Kaltchev et al "Lattice Studies for a High Brightness Light Source" PAC 1995.**

Lessons Learnt, SLS: Seven-BA-6 -> TBA-12

G. Mülhaupt et al (NIM 404, 1998)

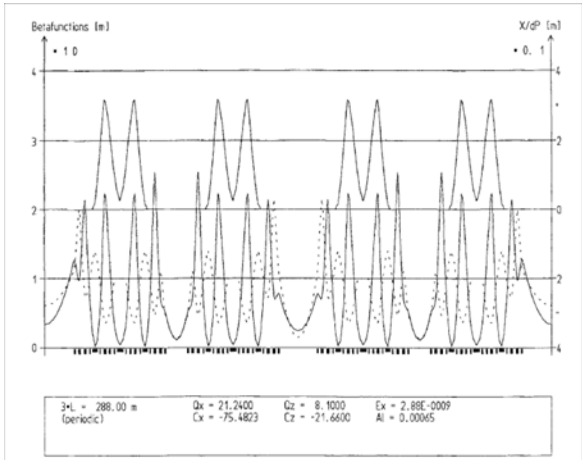

Fig. 1. Linear optics of one-third of the ring. The tune advances over one TBA cell (including the halves of the adjacent straights) are $\Delta\nu_x = 1.77$ and $\Delta\nu_y = 0.64$ for the first cell and $\Delta\nu_x = 1.77$ and $\Delta\nu_y = 0.71$ for the second cell for approximate cancellation of h_{20001} and h_{00201} over the short straights. The sum tune advances of both cells are $\Delta\nu_x = 3.54$ and $\Delta\nu_y = 1.35$, so that their mirror image approximately cancels the five geometric modes over the medium straight.

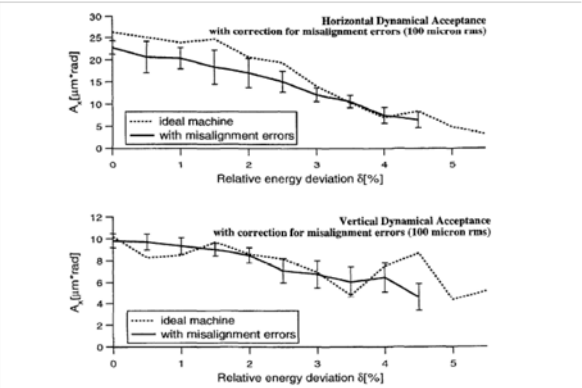

Fig. 3. Transverse dynamic acceptances of the lattice as a function of momentum deviation, including synchrotron oscillations. Transverse acceptances are calculated as the area of an phase-space ellipse, fitted to the Poincaré plot of the outermost particle found to be stable over 512 turns, corresponding to six periods of synchrotron oscillation. An ideal cavity of 6 MV overvoltage producing a rather large synchrotron tune of 0.012 had been assumed for this lattice study in order not to be limited by the RF-acceptance. The geometric acceptance limitations from the elliptic vacuum chamber with 60 mm width and 35 mm height are given by 35 μm rad for the horizontal and 14 μm rad for the vertical.

A. Streun et al (PAC01)

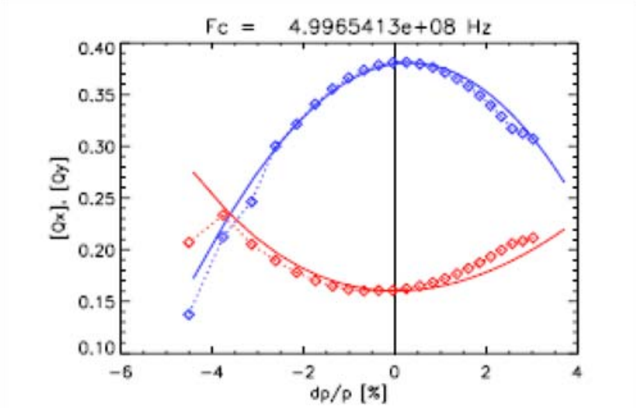

Figure 2: Fractional tunes as a function of relative momentum deviation. A frequency variation of +10/-12 kHz translates to a momentum deviation of -4.7/+3.0 % due to the large nonlinear momentum compaction: $\alpha_o = 6.5 \cdot 10^{-4}$, $\alpha_1 = 4.6 \cdot 10^{-3}$. The solid lines show the TRACY [3] simulation, the diamonds are measurements, upper curve (blue) is horizontal.

This level of agreement between model & measurements is expected; for single particle dynamics. A matter of a first principles approach.

Closing-the-Loop: Beam Studies (2007)

A. Streun et al 2009

Resonance guesses

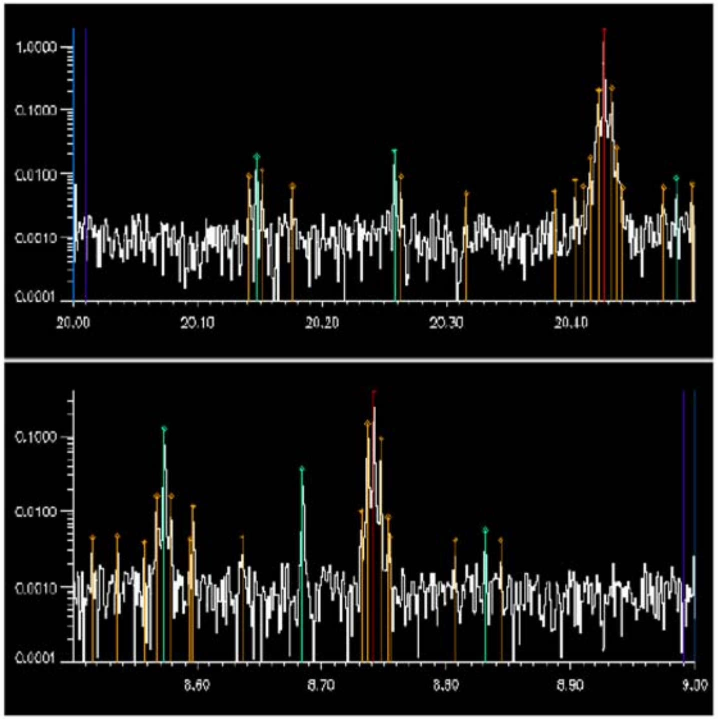

example: set

$$h_{10020} = 6 \cdot 10^{-9} \cdot e^{2\pi/3}\ m^2$$

with auxiliary sextupoles and pinger magnets

↓

try to identify resonances

$$aQ_x + bQ_y = n$$

	peak [mm]	Tune	Guess	min.dist.	[a	b	n]
X	1.83895	20.42643					
3	0.02222	20.25797	20.25803	-0.000003	[1	-1	12]
4	0.01860	20.14714	20.14714	0.000001	[3	0	61]
9	0.00845	20.48409	20.48394	0.000039	[1	-2	3]
Y	0.39925	8.74197					
1	0.12353	8.57357	8.57357	-0.000000	[1	-1	12]
3	0.03584	8.68453	8.68446	0.000017	[1	-2	3]
9	0.00554	8.83162	8.83160	0.000005	[1	2	38]

1000 turn FFT
sine window
peak interpolation

A. Streun, PSI   NLBD-II, DIAMOND, Nov 2-4, 2009   11

Closing-the-Loop (2009)

A. Streun et al 2009

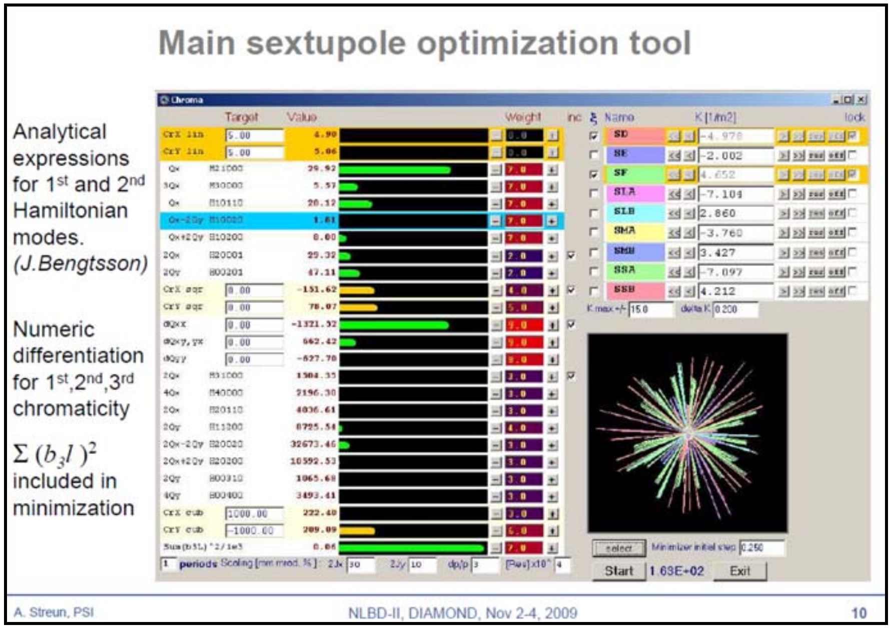

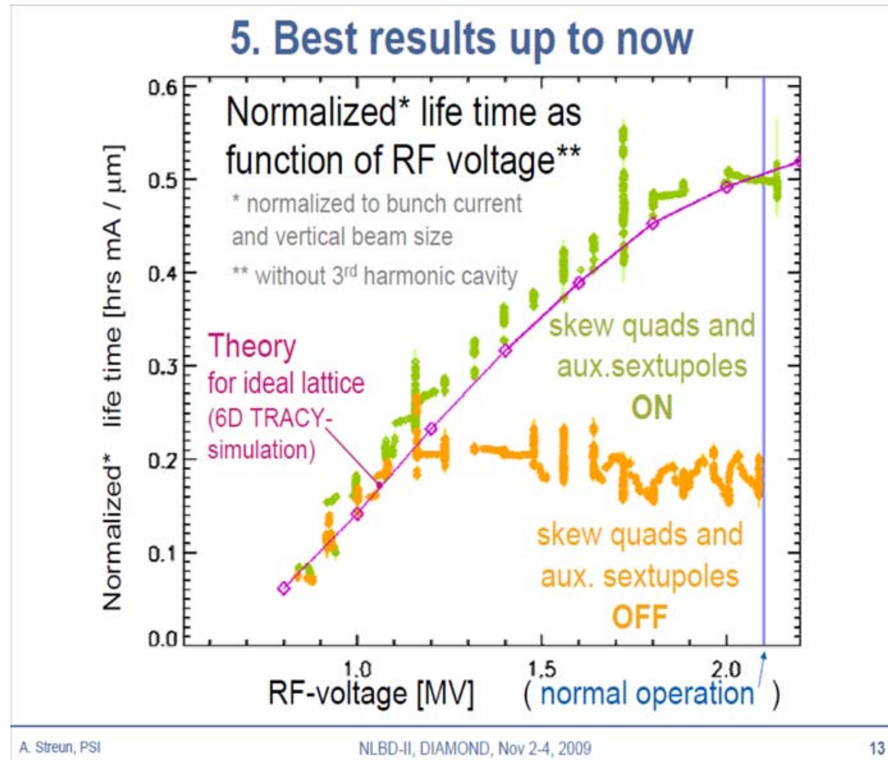

Observation, SOLEIL: Alpha Buckets

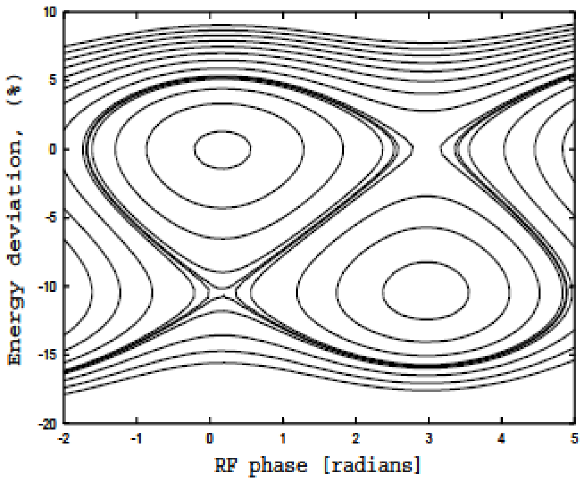

D. Robin, E. Forest, C. Pellegrini, A. Amiry "Quasi-Isochronous Storage Rings" Phys. Rev. E 48 (1993).

$$\alpha_c^{(1)} \sim \frac{1}{\nu_x^2}$$

SOLEIL PAC 1999; validation by 6D phase-space tracking.

$$H(\phi, \delta; s) = \frac{\eta^{(1)} h\omega_0}{2c_0}\delta^2 + \frac{\eta^{(2)} h\omega_0}{3c_0}\delta^2 + \frac{\omega_0 eV_{rf}}{2\pi c_0 E_0}(\cos(\phi + \phi_s) + \phi\sin(\phi_s))$$

$$\phi' = \partial_\delta H = \frac{h\omega_0\eta^{(1)}}{c_0}\delta + \frac{h\omega_0\eta^{(2)}}{c_0}\delta^2, \qquad \delta' = -\partial_\phi H = \frac{\omega_0 eV_{rf}}{2\pi c_0 E_0}(\sin(\phi + \phi_s) - \sin(\phi_s))$$

NSLS-II: Initial Concept (EPAC 2003)

Linear scaling of SLS:

TBA-12, C = 288, = 5.5 nm·rad @ 2.4 GeV

to "2×SLS":

TBA-24, C = 523 m @ 3.0 GeV

gives

$$\varepsilon_x = \left(\frac{3.0}{2.4}\right)^2 \cdot \frac{1}{2^3} \cdot 5.5 = 1.1 \text{ nm·rad @ 3.0 GeV}$$

However, dynamic aperture does not scale: $\hat{\eta}_x \sim \phi_b$ (J. Bengtsson EPAC 2006).

S. Kramer, J. Bengtsson "Optimizing the Dynamic Aperture for Triple Bend Achromatic Lattices" EPAC 2006.

S. Krinsky, J. Bengtsson, S. Kramer "Consideration of a Double Bend Achromatic Lattice for NSLS-II" EPAC 2006.

S. Ozaki, J. Bengtsson, S. Kramer, S. Krinsky, V. Litvinenko "Philosophy for NSLS-II Design with Sub-Nanometer Horizontal Emittance" PAC 2007.

NSLS-II: Lattice Evolution

TBA-24 EPAC 2004

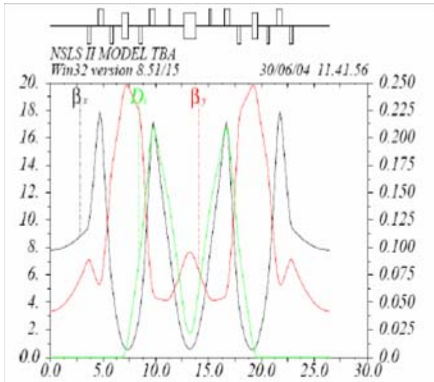

Figure 4: TBA Cell for NSLS II Ring

TBA-24 EPAC 2006

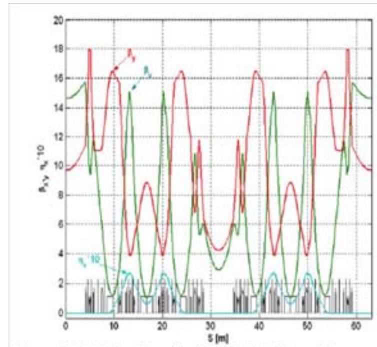

Figure 3: Beta functions for the ETBA lattice with $\varepsilon_x = 2.24nm$, $(\nu_x, \nu_y) = (1.345, 0.616)/cell$, $(\xi_x, \xi_y) = -2.09, -1.15/cell$, and $C = 758m$.

DBA-30+4 DWs EPAC 2006

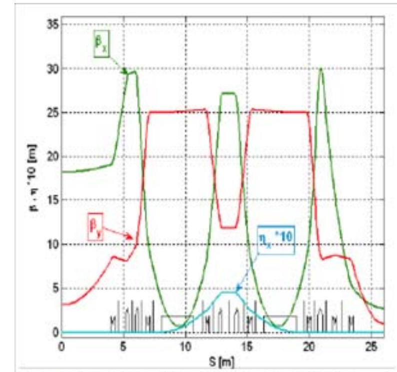

Fig. 1 The lattice functions for one DBA cell. A superperiod is comprised of this cell plus its reflection about the insertion center.

J. BengtssonEPAC06

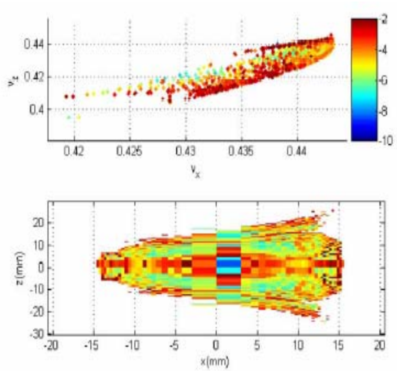

Figure 2: Frequency Map[5] for the Original TBA-24 Cell ($\beta_x = 3.0\,\text{m}, \beta_y = 5.5\,\text{m}$).

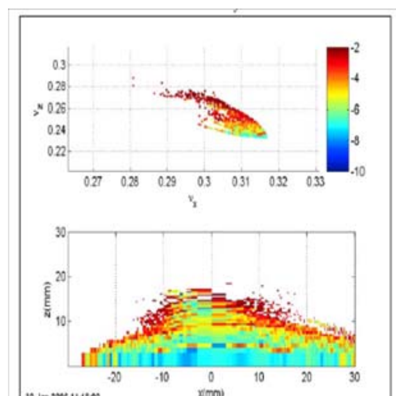

Figure 5: Frequency diffusion map (period tune) and DA for the ETBA in high beta ID straight ($\beta_x = 14.6, \beta_y = 9.7m$).

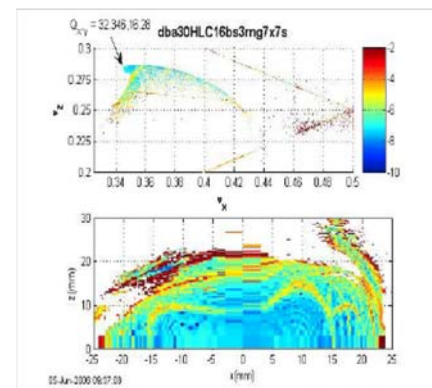

Figure 3: The frequency diffusion map (ring tune) and DA for the DBA(15x2) lattice using 11 sextupole families.

$\left|\frac{\bar{\xi}}{\text{Cell}}\right| = [3.8, 1.2]$, $C = 630$ m $\left|\frac{\bar{\xi}}{\text{Cell}}\right| = [2.1, 1.1]$, $C = 758$ m $\left|\frac{\bar{\xi}}{\text{Cell}}\right| = [3.3, 1.4]$, $C = 780$ m

NSLS-II: Parametric Evaluation (CDR, 2006)

Table 4.2.3 Storage Ring Parameters for Number of DBA Lattice Cells Varying from 32 to 24.

Lattice	DBA32	DBA30	DBA28	DBA26	DBA24
Circumference [m]	822	780	739	697	656
Bend magnet radius [m]	25	25	25	25	25
Straight sections [n x (m)]	16x(8, 5)	15x(8, 5)	14x(8, 5)	13x(8, 5)	12x(8, 5)
Horizontal emittance, ε_x (bare) [nm-rad]	1.7	2.1	2.6	3.2	4.1
Horizontal emittance, ε_x (full set of damping wigglers) [nm-rad]	0.5	0.6	0.7	0.8	1.1
Straight Section Utilization					
8 m straights					
RF and injection	3	3	3	3	3
Damping wigglers	8	8	8	8	8
Undulators	5	4	3	2	1
5 m straights					
Undulators	16	15	14	13	12

- $\varepsilon_x^{\mathrm{IBS}} = 0.2 - 0.25\ \mathrm{nm \cdot rad}$.
- ***C***: ~$1 M per m.

NSLS-II: Parametric Evaluation (CDR, 2006, cont.)

Figure 6.1.2 The fractional reduction of the ring emittance and the increase in energy spread for dipole magnets of bend radii: ρ_o = 25 m (proposed for NSLS-II) and ρ_o = 16.7 m dipole that could yield a shorter circumference lattice.

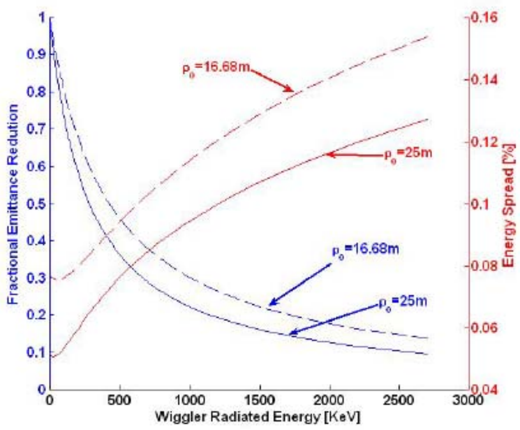

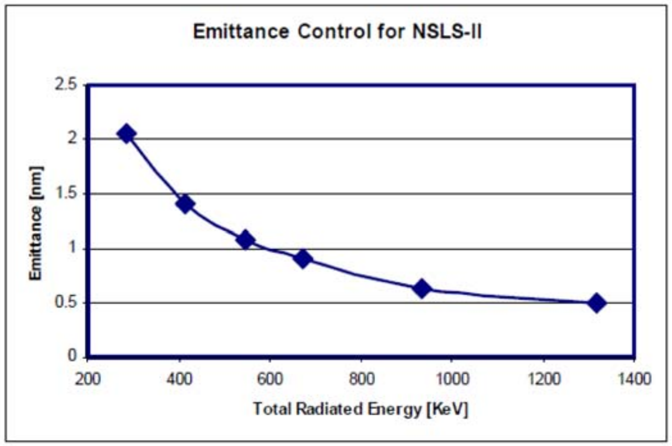

Figure 6.1.3 Emittance reduction for NSLS-II as 0, 1, 2, 3, 5, and 8 DW (7 m each) are installed and operated at 1.8 T peak field.

Table 6.1.3 Effect of Three and Eight 7 m Damping Wigglers on Beam Properties at 3 GeV.

	Zero DWs	Three 7 m DWs (21 m)	Eight 7 m DWs (56 m)
Energy loss [keV]	287	674	1320
RF voltage (3% bucket) [MV]	2.5	3.1	3.9
Synchrotron tune	0.0079	0.00876	0.0096
Natural emittance: ε_x, ε_y [nm-rad]	2.1, 0.01	0.91, 0.008	0.50, 0.005
Damping time: τ_x, τ_s [ms]	54, 27	23, 11.5	12, 6
Energy spread [%]	0.05	0.089	0.099
Bunch duration [ps]	10	15.4	15.5

Virtual Accelerator (J. Rowland, DIAMOND, PAC 2005)

Connect EPICS to a virtual accelerator simulated with Tracy-3 by Virtual IOCs; aka J.M.S. (James' Model Server).

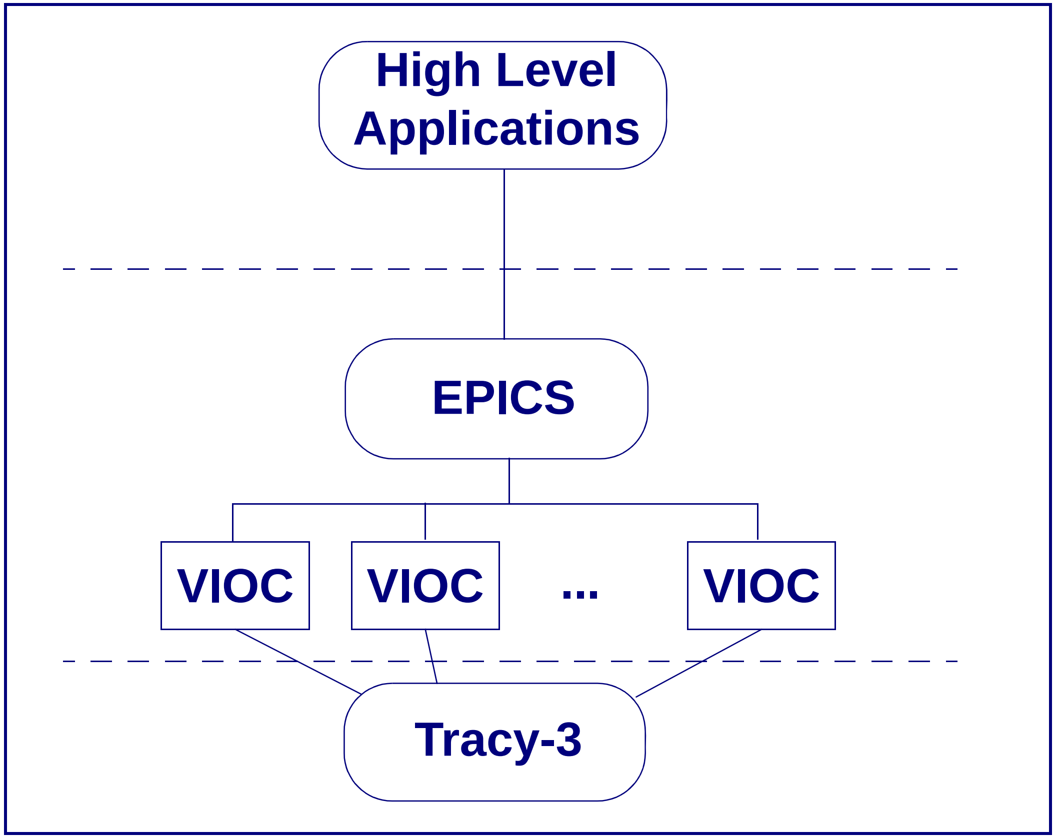

Closing-the-Loop (M. Böge, SLS, PAC 2001)

- **Re-use accelerator design model (Tracy-2) as on-line model: by machine translating (with p2c) ~10,000 lines of Pascal code to C.**
- **Feasible because the code is organized as a library and the internal beam dynamics model is: architectured, layered, and recursive.**

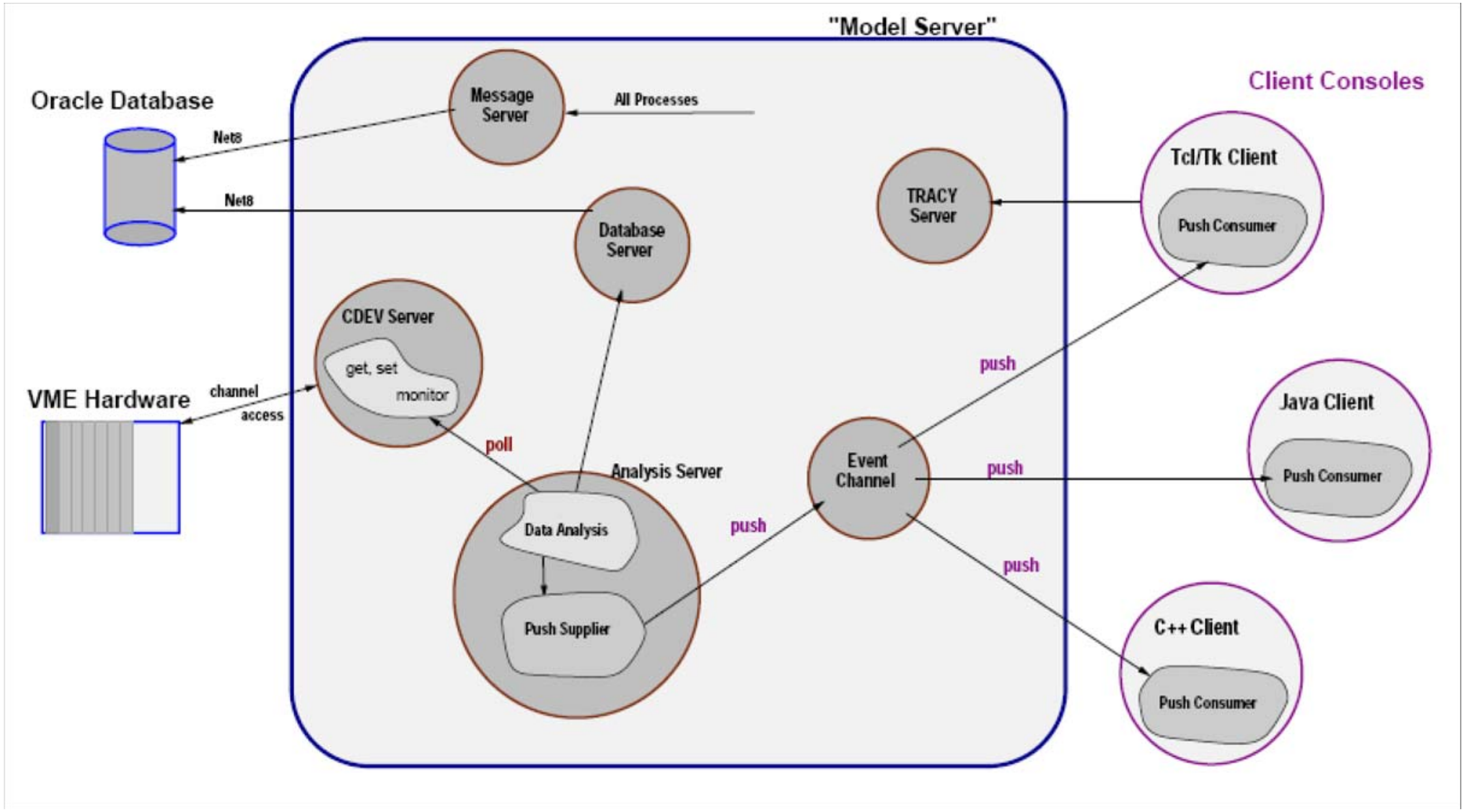

Model Based Control by Thin Clients (CD2, 2007)

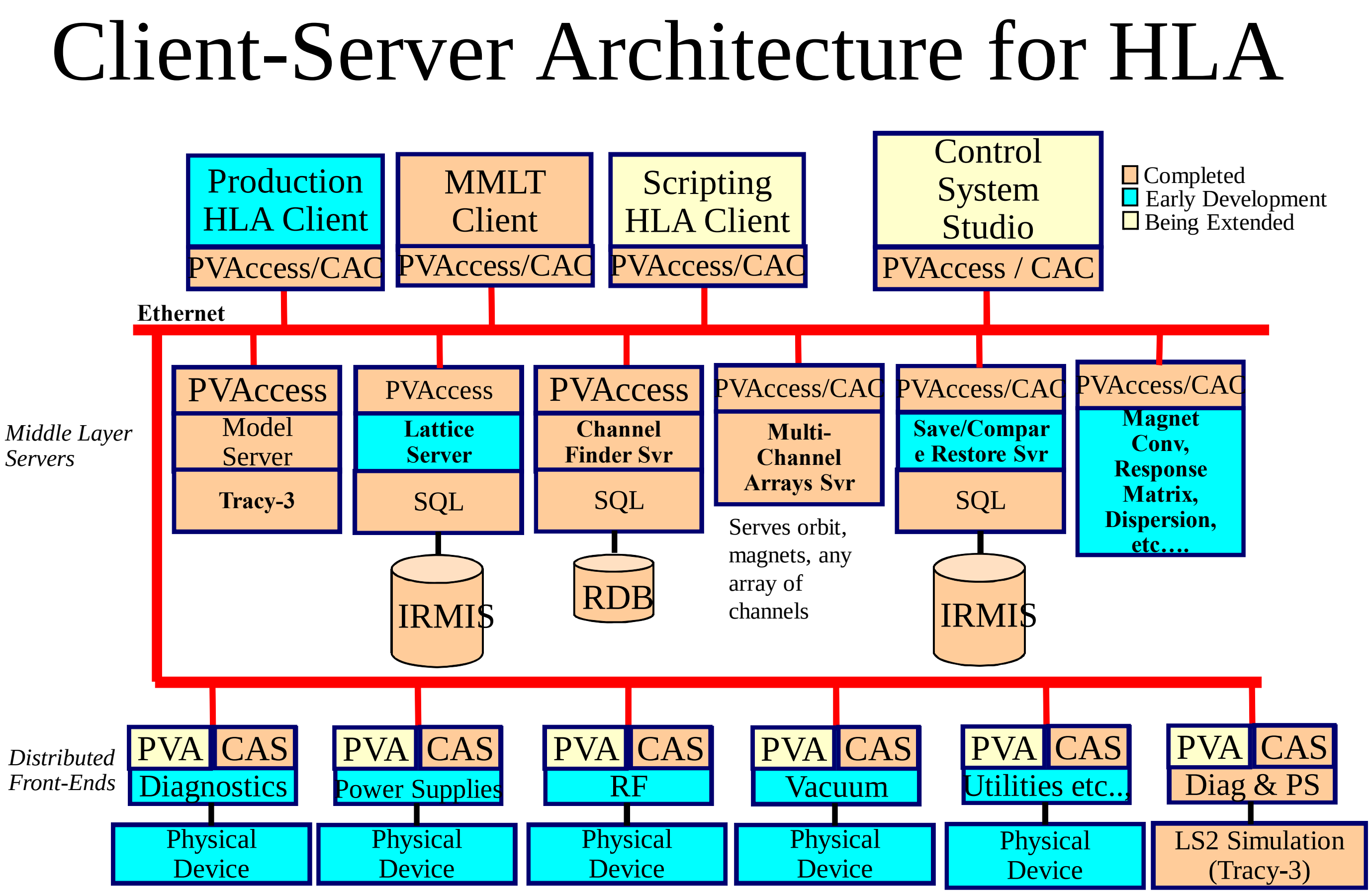

- **In collaboration with B. Dalesio.**

Improved by G. Shen et al (PAC 2011): Name Srv, Twiss Srv, etc.

NSLS-II: Storage Ring Commissioning (APS, 2015)

SR COMMISSIONING

NSLS-II Commissioning	
30-Mar-14	1st turn around SR is complete.
31-Mar-14	3 turns complete
3-Apr-14	Wrong kicker polarity is found and fixed. Circulating beam
5-Apr-14	Beam up to 200 turns. Turned on the sextupoles, retuned the BTS/orbit, almost 300 turns. RF is ON. Stored beam 10k+ turns
8-Apr-14	Storing up to about 0.25mA (70% injection efficiency)
16-Apr-14	0.5mA one-shot injection with on-axis injection; Accumulated >2.6mA
23-Apr-14	Local vertical bump in BPMs 62/63 shown an obstacle in vacuum chamber
25-Apr-14	After opening up the 3rd bellows, an RF contact spring was found in cell10.
29-Apr-14	25 mA!
11-May-14	Phase I commissioning complete
11-Jul-14	SC RF is commissioned. 50 mA is accumulated
23-Oct-14	First project beamline's first light
08-Dec-14	Insertion Device and Frond End commissioning complete
01-Apr-15	Beam emittance is 1 nm rad and 7 pm rad

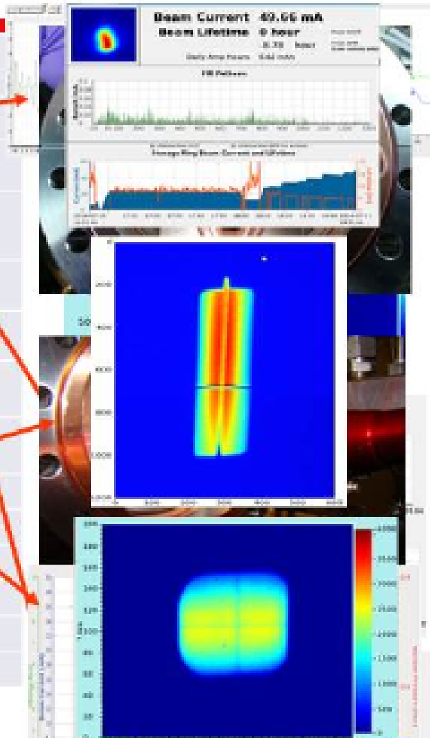

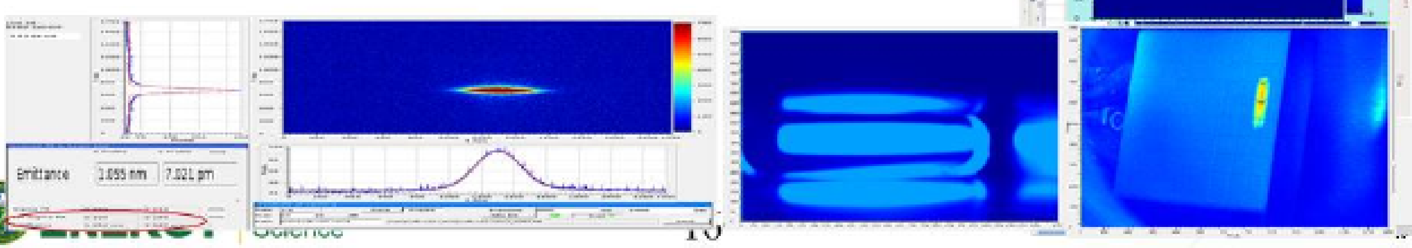

NSLS-II: Predictable Results (APS, 2015)

NSLS-II Design Parameters: High current

Parameters	Design	Measured
Beam Energy [GeV]	3	3
Beam Current [mA]	500	100
Horizontal Emittance [nm-rad]	1	1
Vertical Emittance [pm-rad]	8	7
Beam transverse Stability [beam size]	10%	<10%

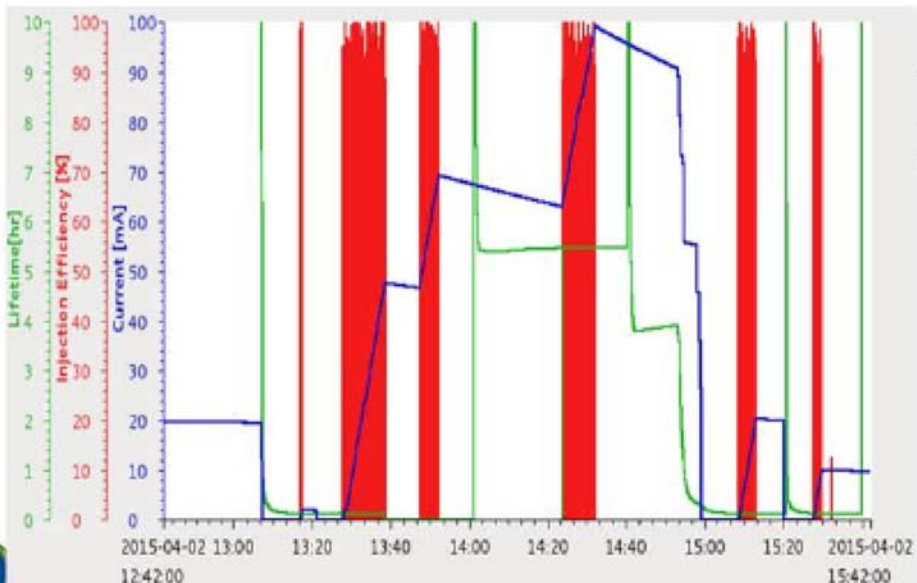

- 100 mA with all IDs closed
- Injection efficiency was > 90%.
- Beam lifetime is ~4 hrs.

BROOKHAVEN NATIONAL LABORATORY

NSLS-II: Predictable Results (APS, 2015)

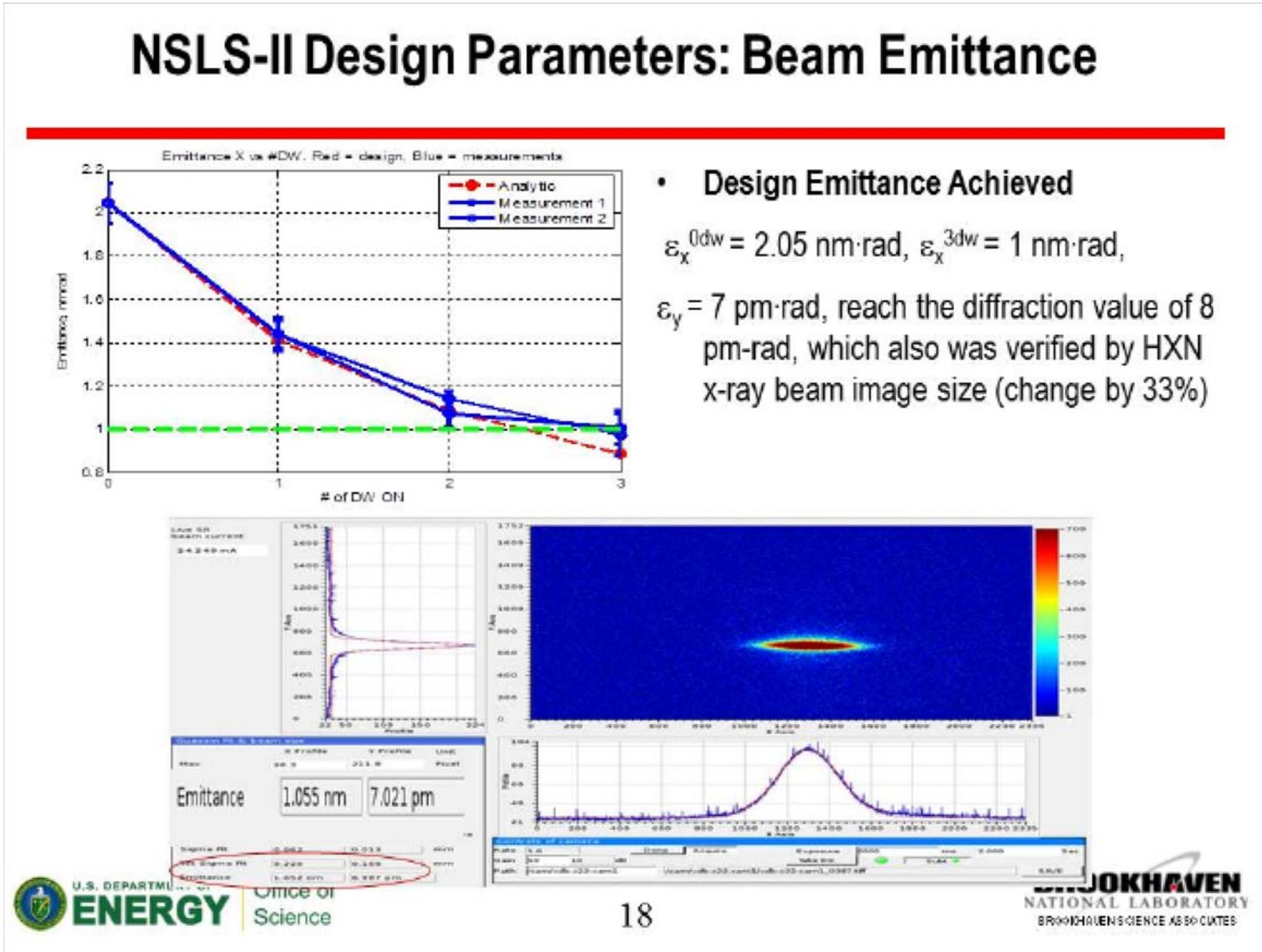

“Outside the Box”: MAX User Mtg 2008 (M. Eriksson)

MAX IV – Swedish / Nordic / Baltic SR facility

1. Small magnets => strong lenses => short magnets
But: How to do it? Never done before.

Ask Lars Johan Lindgren and Bengt Anderberg!

2. But you need new types of lattices?

Ask Simon Leeman, Johan Bengtsson (Brookhaven) and Andreas Streun (PSI) to develop codes and number-crunch!

3. The vacuum chamber bore is to small for pumping?

Ask Erik Wallén, Magnus Berglund. Anders Hansson and Roberto Kersevan (ESRF) to develop and characterize a linear pumping system (NEG-coated)!

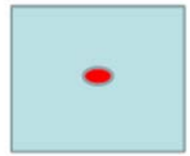

MAX IV magnet
with vacuum tube

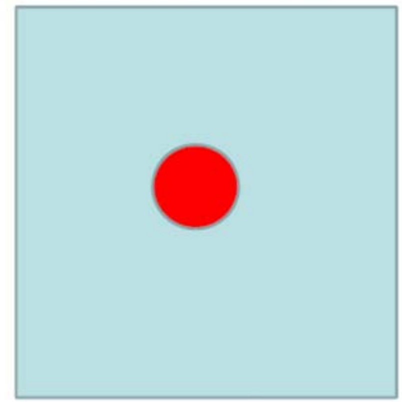

Conventional magnet
with vacuum tube

4. Ultra-small emittance=>no beam life-time!

Ask Lars Malmgren, Per Lilja, Robert Nilsson, Åke Andersson to make 100 MHz RF system with huge energy acceptance!

MAX-lab

MAX User Meeting 2008

Question: What is fundamentally different from previous designs?

Pushing the Envelope: MAX-IV Seven-BA-20

Ignore TME, instead, focus on $1/N^3$. Provide space (by innovative magnet design). Introduce octupoles to improve (=> direct) control of the second order sextupolar driving terms (M. Eriksson et al PRST-AB 12, 120701, 2009).

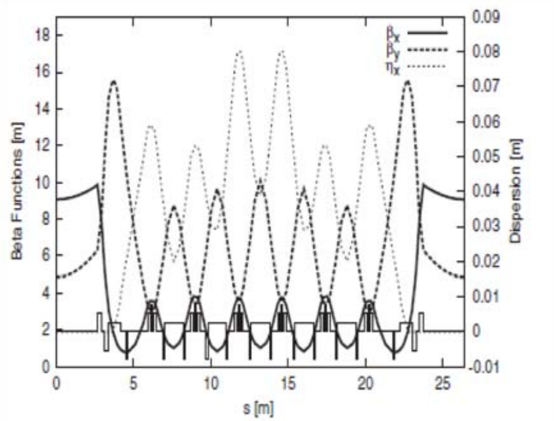

FIG. 2. Beta functions β_x, β_y and dispersion η_x for one achromat of the 3 GeV storage ring. The position of the dipoles, quadrupoles, and sextupoles are indicated at the bottom.

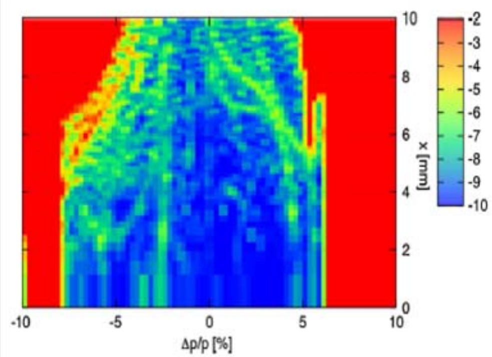

FIG. 12. (Color) Diffusion map taken at the center of the long straight section for off-momentum particles in the 3 GeV storage ring with four PMDWs installed. The scale is logarithmic in tune shift from low (blue) to high (red).

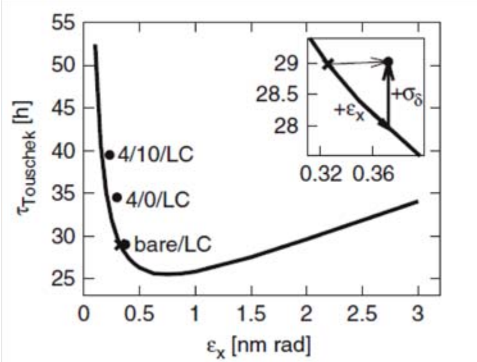

FIG. 15. The trend line shows Touschek lifetime for the bare lattice (IBS neglected) if it were possible to vary the lattice emittance while keeping the energy spread constant. Specific configurations (bare lattice, four PMDWs, and four PMDWs plus ten IVUs; all including LCs) are indicated by crosses and dots. Crosses indicate IBS neglected, dots indicate IBS included. The enlarged segment illustrates the effect of IBS for the bare lattice configuration: while the IBS emittance growth ($+\varepsilon_x$) leads to a decrease of Touschek lifetime, the IBS energy spread growth ($+\sigma_\delta$) leads to an increase of Touschek lifetime.

See also V. Litvinenko FLS 1999

MAX-IV Project Status Report, 2010:

"Committee consider MAX-IV an *innovative and daring project* and concluded that

...DDR (Detailed Design Report) has *addressed all the issues* relevant to achieving the performance goals... tolerance requirements... are demanding but not beyond what is reachable..."

Colliders: The FODO Cell

The linear optics for a FODO cell

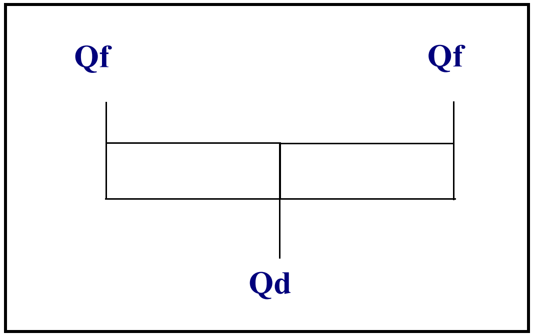

is well known (for $k_{\mathrm{Qf}} = -k_{\mathrm{Qd}}$)

$$\beta_{x\max} = \frac{2\rho\sin(\phi)(1+k\rho\sin(\phi))}{\sin(\mu_x)} \to \frac{2L_{\mathrm{b}}(1+kL_{\mathrm{b}})}{\sin(\mu_x)} + O(\phi^3) = \frac{2L_{\mathrm{b}}\left(1+\sin\left(\frac{\mu_x}{2}\right)\right)}{\sin(\mu_x)} + O(\phi^3),$$

$$\eta_{x\max} = \frac{2\rho\sin^2\left(\frac{\phi}{2}\right)(2+k\rho(2\sin(\phi)))}{\sin^2\left(\frac{\mu_x}{2}\right)} \to \frac{\rho\phi^2\left(1+\frac{1}{2}kL_{\mathrm{b}}\right)}{\sin^2\left(\frac{\mu_x}{2}\right)} + O(\phi^4) = \frac{L_{\mathrm{b}}^2\left(1+\frac{1}{2}\sin\left(\frac{\mu_x}{2}\right)\right)}{\rho\sin^2\left(\frac{\mu_x}{2}\right)} + O(\phi^4)$$

where we have used $\sin\left(\frac{\mu_x}{2}\right) = \pm\frac{kL_{\mathrm{b}}}{2}$.

Colliders: The FODO Cell (cont.)

If it was considered being used for e.g. a damping ring, the hor. emittance would be

$$\varepsilon_x = C_q \gamma^2 \frac{\langle H/|\rho|^3 \rangle}{J_x \langle 1/\rho^2 \rangle},$$

where $\mathcal{H}$ is the linear dispersion action

$$H \equiv \|\tilde{\eta}\| = \tilde{\eta}^T \tilde{\eta}, \qquad \tilde{\eta} \equiv A^{-1}\bar{\eta}, \qquad A^{-1} = \begin{bmatrix} 1/\sqrt{\beta_x} & 0 \\ \alpha_x/\sqrt{\beta_x} & \sqrt{\beta_x} \end{bmatrix},$$

which to leading order is

$$\langle H(s) \rangle = \frac{\rho \phi_b^3}{\sin^3\left(\frac{\mu_x}{2}\right)} \left[1 - \frac{(kL_b)^2}{16}\right] + O(\phi_b^4)$$

and has a min for

$$\Delta\mu_x = 180°, \qquad kL_b = 2, \qquad \langle H(s) \rangle = \rho \phi_b^3 .$$

Colliders: The FODO Cell (cont.)

However, this is a leading order result. An exercise in algebra leads to the rather neat result (Helm, Wiedemann <u>SLAC PEP Note 303, 1973</u>)

$$\langle \mathcal{H}(s) \rangle = \frac{\rho\phi^3}{\sin^3\left(\frac{\mu_x}{2}\right)\cos\left(\frac{\mu_x}{2}\right)}\left(1 - \frac{3}{4}\sin^2\left(\frac{\mu_x}{2}\right) + \frac{1}{60}\sin^4\left(\frac{\mu_x}{2}\right)\right) + O(\phi^5)$$

which has a min for

$$\mu_x = 2\,\mathrm{atan}\left(\frac{1}{2}\sqrt{\frac{75 + 3\sqrt{1905}}{8}}\right) \approx 0.38 \cdot 2\pi, \qquad \langle \mathcal{H}(s) \rangle_{\min} = \frac{1}{60}\sqrt{\frac{16075 + 381\sqrt{1905}}{6}} \approx 1.23 \cdot \rho\phi_b^3.$$

However, a formula is (to our knowledge) not provided for the linear chromaticity. One can show that

$$\xi_x = -\frac{1}{\pi}\tan\left(\frac{\mu_x}{2}\right)$$

and it follows that

$$\xi_x = \begin{cases} -1/\pi, & \mu_x = 90° \\ -0.81, & \mu_x = 137° \end{cases}.$$

"R&D": The OFODOFO Cell

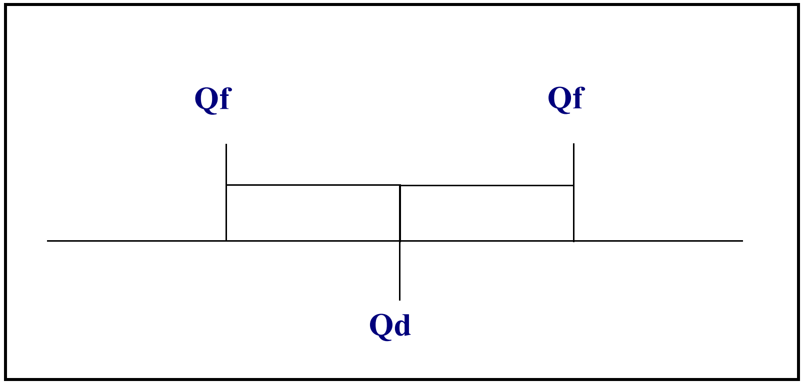

The linear dispersion action has a min for

$$\eta_{xc} = \frac{L_b \phi}{24}, \qquad \eta'_{xc} = 0,$$

$$\alpha_{xc} = 0, \qquad \beta_{xc} = \frac{L_b}{2\sqrt{15}\sqrt{1 - \frac{3}{8}k_d L_b + \frac{3}{80}k_d^2 L_b^2}},.$$

$$\langle \mathcal{H}(s) \rangle_{min} = \frac{L_b \phi^2}{12\sqrt{15}}\sqrt{1 - \frac{3}{8}k_d L_b + \frac{3}{80}k_d^2 L_b^2}$$

“R&D”: The OFODOFO Cell (cont.)

One can also show that

$$\mu_x = 2\,\mathrm{atan}\left(-\frac{3}{\sqrt{15}}\frac{1-\frac{1}{4}k_\mathrm{d}L_\mathrm{b}}{\sqrt{1-\frac{3}{8}k_\mathrm{d}L_\mathrm{b}+\frac{3}{80}k_\mathrm{d}^2L_\mathrm{b}^2}}\right)$$

and

$$\xi_x = -\frac{12}{8\pi\sqrt{15}}\frac{1-\frac{1464}{3072}k_\mathrm{d}L_\mathrm{b}+\frac{254}{3072}k_\mathrm{d}^2L_\mathrm{b}^2-\frac{13}{3072}k_\mathrm{d}^3L_\mathrm{b}^3}{\left(1-\frac{1}{8}k_\mathrm{d}L_\mathrm{b}\right)\sqrt{1-\frac{30}{80}k_\mathrm{d}L_\mathrm{b}+\frac{3}{80}k_\mathrm{d}^2L_\mathrm{b}^2}},$$

$$\begin{aligned}\xi_y = {} & (43008+24672k_\mathrm{d}L_\mathrm{b}-25200k_\mathrm{d}^2L_\mathrm{b}^2+6330k_\mathrm{d}^3L_\mathrm{b}^3-609k_\mathrm{d}^4L_\mathrm{b}^4+20k_\mathrm{d}^5L_\mathrm{b}^5) \\ & /(4\pi\mathrm{sqrt}(-242810880-91594752k_\mathrm{d}L_\mathrm{b}+163349504k_\mathrm{d}^2L_\mathrm{b}^2-15035392k_\mathrm{d}^3L_\mathrm{b}^3-34034880k_\mathrm{d}^4L_\mathrm{b}^4 \\ & 17085840k_\mathrm{d}^5L_\mathrm{b}^5-3894596k_\mathrm{d}^6L_\mathrm{b}^6+500032k_\mathrm{d}^7L_\mathrm{b}^7-37141k_\mathrm{d}^8L_\mathrm{b}^8+1490k_\mathrm{d}^9L_\mathrm{b}^9-25k_\mathrm{d}^{10}L_\mathrm{b}^{10})\end{aligned}$$

"R&D": The OFODOFO Cell - Scaling Laws

The hor linear chromaticity is essentially flat and the vertical has a min for

$$k_{\mathrm{d}} L_{\mathrm{b}} \approx -1.24088$$

which gives

$$k_{\mathrm{d}} \approx \frac{-1.24088}{L_{\mathrm{b}}}, \qquad L_1 \approx 0.88121 \cdot L_{\mathrm{b}}, \qquad k_{\mathrm{f}} \approx \frac{2.86572}{L_{\mathrm{b}}}$$

with

$$\beta_{y\mathrm{c}} \approx 13.1 \cdot L_{\mathrm{b}}, \qquad \nu_x \approx 0.781, \qquad \nu_y \approx 0.220, \qquad \xi_x \approx -1.195, \qquad \xi_y \approx -1.718$$

and the total cell length is

$$L = (1 + 2L_1)L_{\mathrm{b}} \approx 2.76242 \cdot L_{\mathrm{b}}.$$

For an example, we may choose

$$\phi_{\mathrm{b}} = 3°, \qquad L_{\mathrm{b}} = 1.0 \text{ m}, \qquad \rho_{\mathrm{b}} = \frac{L_{\mathrm{b}}}{\phi_{\mathrm{b}}} \approx 19.1 \text{ m}$$

and scale it by a factor 0.1.

Interestingly, the linear chromaticity is not increased.

“R&D”: The OFODOFO Cell - Scaling Laws (cont.)

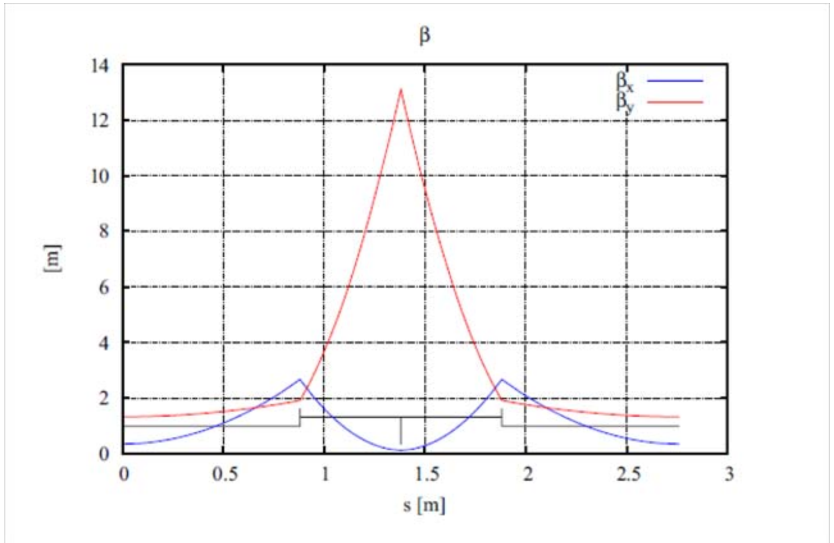

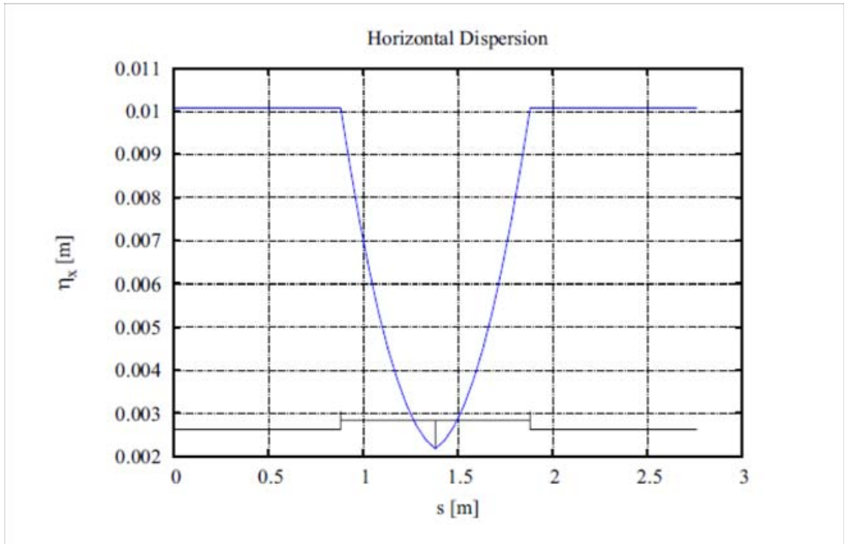

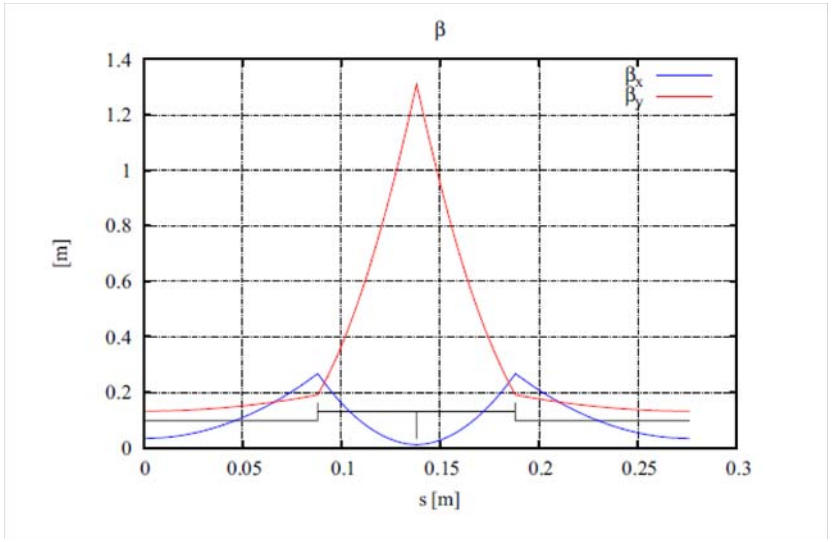

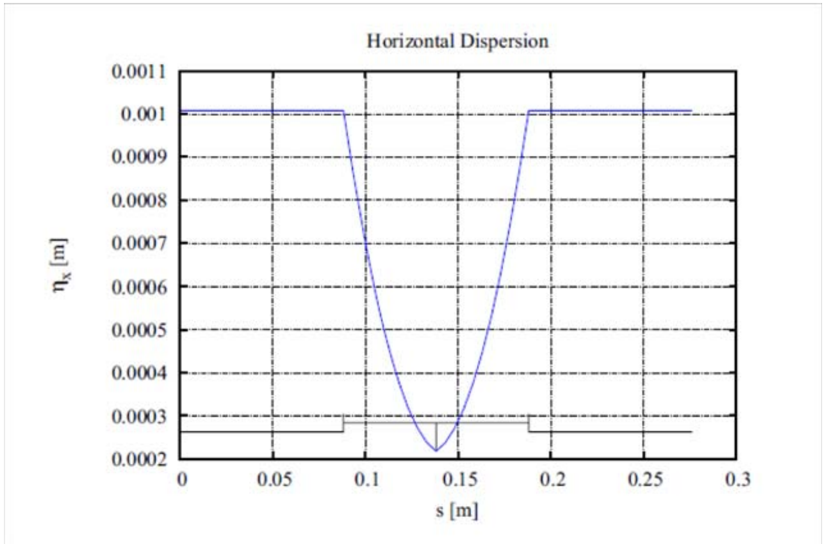

Reality Check: A Min Emittance Cell for MAX-IV

We will now return to our initial example:

$$\phi_{\mathrm{b}} = 3°, \qquad L_{\mathrm{b}} = 1.0 \text{ m}, \qquad \rho_{\mathrm{b}} = \frac{L_{\mathrm{b}}}{\phi_{\mathrm{b}}} \approx 19.1 \text{ m},$$

reduce ε_x by a factor of $\varepsilon_r = 13$ to $\varepsilon_x = 0.615$ nm·rad @3 GeV for minimum hor/ver linear chromaticity, and compare it with the MAX-IV unit cell, i.e., for the same linear dispersion action $\mathcal{H}$.

In particular, the MAX-IV unit cell has $\varepsilon_x = 0.334$ but $J_x \approx 2$ because the Q_d gradient is integrated into the dipole.

3D Parametric Plot of Hor/Ver Linear Chromaticity

$\xi_x(k_{Qd}, \beta_{xc})$

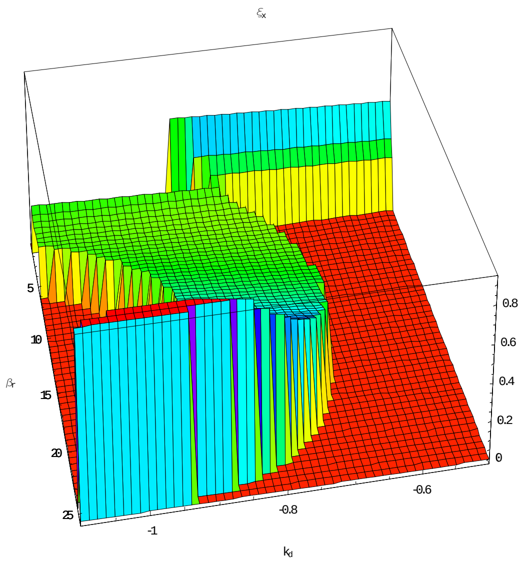

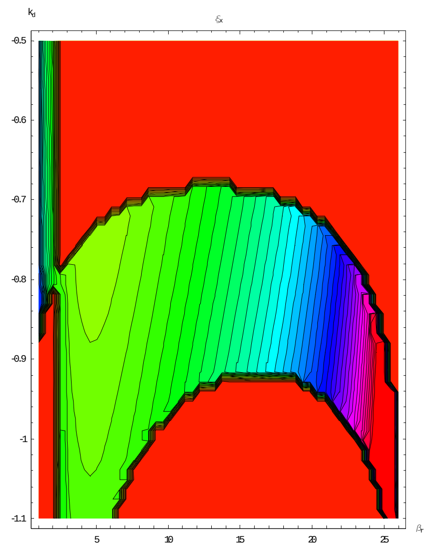

$\xi_y(k_{Qd}, \beta_{xc})$

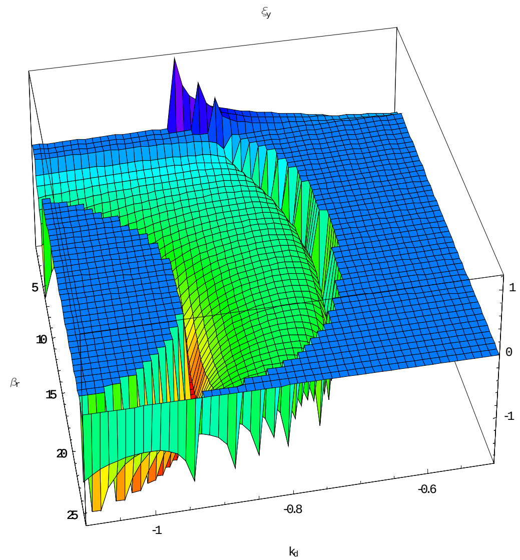

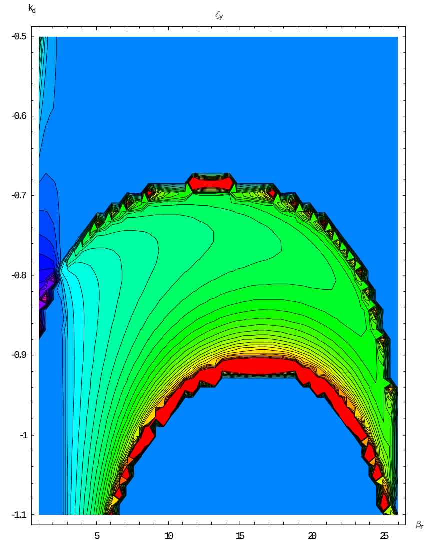

Reality Check: A Min Emittance Cell for MAX-IV (cont.)

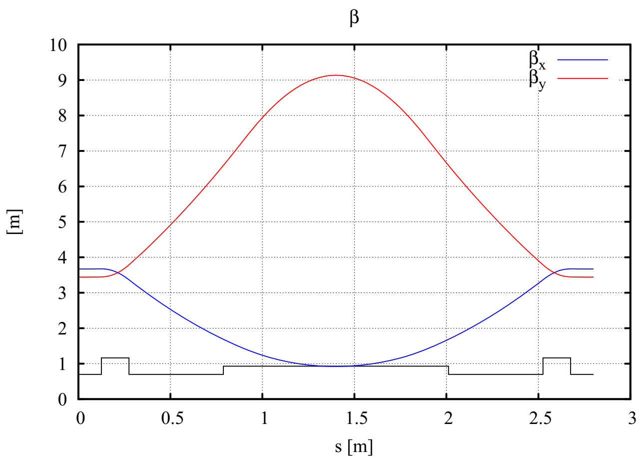

MAX-IV Unit Cell

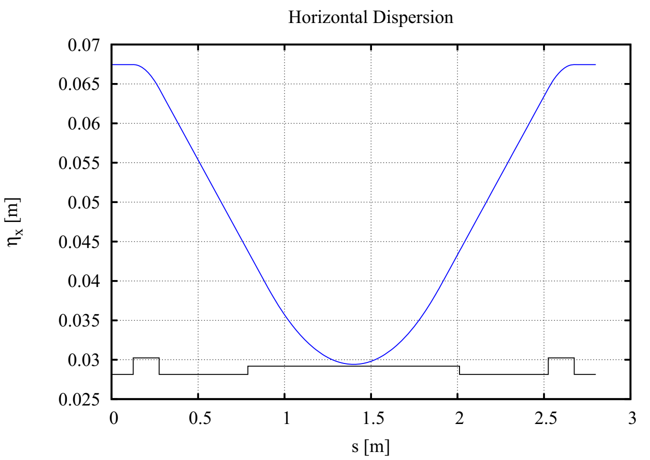

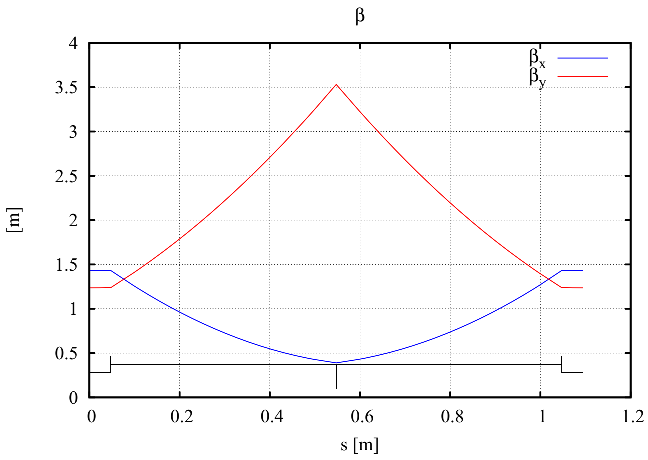

ME Cell

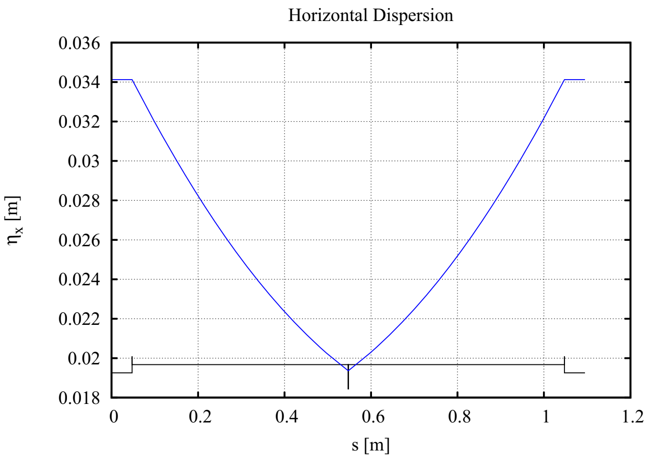

Reality Check: A Min Emittance Cell for MAX-IV (cont.)

The tune and linear chromaticity are

$$\nu_x \approx 0.244, \qquad \nu_y \approx 0.089, \qquad \xi_x \approx -0.232, \qquad \xi_y \approx -0.232$$

whereas the MAX-IV unit cell has

$$\nu_x \approx 0.265, \qquad \nu_y \approx 0.082, \qquad \xi_x \approx -0.270, \qquad \xi_y \approx -0.241 .$$

To summarize, the MAX-IV unit cell it is well (numerically) optimized for the given parameters.

It can be scaled according to the scaling properties summarized on slide 32, with-out affecting the linear chromaticity; but the peak beta functions and hor linear dispersion will change.

Conclusions

- Hamiltonian dynamics, perturbed by classical radiation and quantum fluctuations, and related numerical and analytical methods provide the foundation for self-consistent, realistic modeling of modern ring-based synchrotron light source.
- In other words: predictable results.
- Applications include: conceptual design, engineering design, simulation of the accelerator for testing and validation of controls algorithms (aka "high level applications"), and model based control for commissioning.

Thank You.